INSTITUTO POLITÉCNICO DE BRAGANÇA
Escola Superior de Tecnologia e Gestão

The Study of Cell Behaviour using Biomedical Microdevices

Vera Luísa Carreira Faustino

Final Project Report to the **Escola Superior de Tecnologia e Gestão**

Instituto Politécnico de Bragança

To obtain Master degree in **Tecnologia Biomédica**

October 2012

INSTITUTO POLITÉCNICO DE BRAGANÇA
Escola Superior de Tecnologia e Gestão

The Study of Cell Behaviour using Biomedical Microdevices

Vera Luísa Carreira Faustino

Final Project Report to the Escola Superior de Tecnologia e Gestão
Instituto Politécnico de Bragança
To obtain Master degree in **Tecnologia Biomédica**

Advisors:
Rui Lima
Gyeong Man-Kim

Co-advisors:
Sergio Arana
Isabel Ferreira

This Final Project Report was a collaboration of the University of Navarra and research centre, CEIT

October 2012

“A person who never made a mistake never tried anything new.”

Albert Einstein

Acknowledgments

The author acknowledge the support provided by: Student Mobility Placements with the program Lifelong Learning (Erasmus Program), PTDC/SAU-BEB/108728/2008, PTDC/SAU-BEB/105650/2008, PTDC/EME-MFE/099109/2008 and PTDC/SAU-ENB/116929/2010 from the FCT (Science and Technology Foundation), QREN, European Union (FEDER) and COMPETE, Portugal and to the Polytechnic Institute of Bragança that assigned the scholarship for the elaboration of master thesis with cooperation of CEIT, University of Navarra, San Sebastian, Spain.

I want to thanks too:

To my advisors and co-advisors, Geong Man Kim, Rui Lima, Isabel Ferreira and Sergio Arana, all the support and knowledge that they share with me.

To PhD student Trang, Post-doctor Ricardo Calhelha and MsC Diana Pinho for help me with patience and sharing every idea for a better work.

To my friends Raquel Rodrigues, Susana Novais, Nuno Pereira and Mario Espinoza the biggest thanks for all the talks, smiles, tears, ideas and friendship, along this journey.

To My parents, my brother and all my family, without them this opportunity would not have been possible; without they support on this stage everything have been much more difficult.

And to João Carvalho for never letting me give up and insist that I am a genius.

Abstract:

The cell culture has become over the years an important discipline for the thorough knowledge of cells behaviour and migration, as also cell-cell interaction. A few years ago it was only possible to create culture systems *in vitro* systems, however, with the advance of new technologies it has become possible to create culture systems *in vivo* closer to reality.

The microfabrication processes such as photolithography were used in this work for the design of a microdevice which is aimed to study the migration of cells into nanofibers.

Beyond the cell studies, microdevices were also used for rheological studies. The behaviour of blood cells is very important, regarding the transport of oxygen in our body as well as nutrients. The knowledge about the factors that influence changes in mechanical properties of erythrocytes is of great importance because it is their deformability that allows them to carry oxygen and pass through smaller arteries and veins. Therefore, another microdevice was used for the purpose of observing the deformation of the erythrocytes after contact with human tumour cell lines (NCI-H460-non-small cell lung cancer and HCT-15 - colon carcinoma) up to two consecutive days. With the flow rate of 500 nl/min, the flowing erythrocytes through the microchannel were captured by a high speed camera and their deformability was examined. The erythrocytes that contacted tumour cells show less deformability than "healthy" erythrocytes.

It was found that the tests were insufficient to conclude clearly the effect of the tumour cells in the deformation of erythrocytes. We have found evidence that erythrocytes also influence the growth of tumour cells, however, further testing would be needed to clarify this observation.

Keywords: Biomedical devices, nanofibers, cell culture, erythrocytes, cancer cells, deformability

Resumo:

A cultura de células tornou-se ao longo dos anos uma importante disciplina para o conhecimento profundo do seu comportamento, migração e interação entre células. Com o avanço de novas tecnologias tornou-se possível criar sistemas de cultura *in vivo* mais próximos da realidade, quando anteriormente apenas existiam sistemas *in vitro*.

Neste trabalho, foram aplicados processos de microfabricação, nomeadamente a fotolitografia, para a conceção de um microdispositivo que teve como objetivo principal o estudo da migração de células em nanofibras.

Para além de estudos celulares, os microdispositivos também foram usados em estudos reológicos. O comportamento do sangue é muito importante, pois é ele que transporta o oxigénio no nosso organismo assim como nutrientes. Perceber o que influencia a alteração das características mecânicas dos eritrócitos é de grande importância pois é a sua deformabilidade que lhes permite transportar o oxigénio e passar nas artérias e veias mais pequenas. Assim, utilizou-se um outro microdispositivo, com o propósito de observar a deformação dos eritrócitos após contacto com linhas celulares tumorais humanas (NCI-H460 – cancro do pulmão e HCT-15 – carcinoma do cólon) até um máximo de dois dias consecutivos. Os eritrócitos fluíram pelo microcanal com uma taxa de fluxo de 500 nl/min e foram capturados por uma câmara de alta velocidade para ver a sua capacidade de deformação. Os eritrócitos que estiveram em contacto com as células tumorais revelam menos deformação que os eritrócitos "saudáveis".

Verificou-se que os ensaios realizados foram insuficientes para concluir com clareza o efeito das células tumorais na deformação dos eritrócitos. Encontraram-se também indícios de os eritrócitos influenciarem o crescimento das células tumorais, no entanto, mais ensaios também seriam necessários para clarificar essas observações.

Palavras-chave: Dispositivos biomédicos, nanofibras, cultura de células, eritrócitos, células cancerígenas, deformação

Table of contents

List of abbreviations

2D – two dimensional/dimension

3D – three dimensional/dimension

ADSC – Adipose-derived stem cells

CEIT – Center studies of technical investigations

DI – Deformation Index

ECM – extracellular matrix

FTIR – Fourier transform infrared spectroscopy

HA – Hydroxyapatite

HBSS – Hank's Balanced Salt Solution

Hct - Hematrocit

MIMIC – micromolding in capillaries

PCL – Poly(ε-caprolactone)

PDMS – Poly (dimethylsiloxane)

PEG – Polyethylene glycol

PGA – Poly(glycolic acid)

PLA – Poly(lactic acid)

PLGA – Polylactide-co-glycolide

PMMA – poly (methylmethacrlate)

RBCs – red blood cells

REM – replica moulding

RPMI – Roswell Park Memorial Institute

SAM – self-assembled monolayer

SAMIM – solvent-assisted micromolding

SEM – Scanning electron microscopy

SFB – Serum Fetal Bovine

UV – ultraviolet

WBCs – white blood cells

μTM – microtransfer moulding

List of figures

List of tables

Chapter I - Background

1. Objectives and motivation

Over the years, cell culture has become an important discipline for the thorough knowledge of their behaviour, migration and cell-cell interaction. With the advance of new technologies, it has been possible to create live culture systems in approximate reality. The cell cultures are made using means which feed the cells and flasks suitable for this purpose. However, the cultures are static and often not accurately reflect the conditions of the cells in a living organism.

Thus, microdevices obtained by microfabrication processes such as photolithography, emerged as good examples of new methods for studying cells both individually and together. There are many types of microdevices for toxicological studies, migration and cell individualization. Having in mind the purpose of performing studies in similar conditions to human body, new scaffolds for culture cells and tissues have been developed, namely nanofibers. Nanofibers are polymeric matrices that have as main objective to serve as support cells. So their material should have the following features: biocompatibility and biodegradability.

Besides cell studies, microdevices are also used for rheological studies. The behaviour of blood cells is very important, regarding its function carrying oxygen in our body as well as nutrients. The knowledge about the factors that influence the change in mechanical properties of erythrocytes is of great importance because it is their deformability that allows them to carry oxygen and pass smaller veins.

Herein, a device was created in order to study the migration of cells in the nanofibers. Several tests were made to assess its viability and various techniques were used to achieve the objective.

Another microdevice was used with the purpose of study the deformation of the erythrocytes, after contact with tumour cell lines (NCI-H460 - non-small cell lung cancer and HCT-15 - colon carcinoma) up to two consecutive days. With the flow rate of 500 nl/min, the flowing erythrocytes through the microchannel were captured by a high speed camera and their deformability was examined. The images were processed and the data taken with Image Analyzer (ImageJ, developed by the National Institute of Health, USA).

2. Cell Culture

Since the moment in which it was possible to differentiate and culture animal cells, the cell research has been growing and has great importance. This advances enabled the study of diseases such as cancer and of advances to treat them.

Animal cell culture began in 1907 by Ross Harrison, but only between 1940's and 1950's became an important tool for scientists due some developments that are now part of procedures (Ryan, 2008).

Cell cultures are described based on two parameters: origin of the cells and manner of growth (suspension or adherent growth). The origin of the cells can be:

- Primary cell culture (from animal or plant tissue) – cells derived directly from tissue and usually die after 50 divisions. These cells may give rise to a cell strain (a lineage of cells originated from one primary culture) or be immortalized (Ryan, 2008);
- Extended culture (multi passage culture – cell strain) – when the cells in the primary culture vessel have grown and filled up all of the available culture substrate; they must be subcultured to give them more room for continue growth (Ryan, 2008);
- Established (transformed) cell lines.

The immortalized cells have some advantage over mortal cells: grow indefinitely in culture and "do not die".

Cells grown in suspension proliferate without the attachment to culture container. Blood, spleen and bone marrow are some examples. Adherent cells grow as a monolayers attached to the surface of culture container. Fibroblasts, epithelial cells or neurons are examples of culture cells.

Cell culture required the following materials (Figure 1):

- Medium (nutrients, Serum Fetal Bovine- SFB, growth factors, amino acids);
- Containers with special treatment to adhere cells;
- Incubator (CO_2+air+H_2O);
- Tissue culture hood.

Figure 1: Some material used in cells culture: A – flasks; B – microplates.

The microsystems dedicated for cell engineering should assure optimal growth of cells, control of cells migration, adhesion and should also provide optimal oxygenation and flow of culture medium (Khademhosseini et al., 2005; Prokop et al., 2004).

In order to precisely study cell physiology and functions as well as their response to various culture conditions, a physiologically meaningful, well-defined and homogenous culture environment is crucial (Wu et al., 2008).

2.1. Cell Migration

Cells sense and respond to a wide variety of external physiological and chemical signals, integrate such complex incoming signals, and change their morphology, dynamics, behaviour, function, and fate (Geiger, Spatz and Bershadsky, 2009). Cell movement is one of the fundamental features of living cells. For example, epithelial cells migrate during wound healing processes, leukocytes migrate to sites of inflammation and infection, vascular endothelial cells migrate to form new capillaries during angiogenesis, and cell sheets migrate to form tissues and organs during development (Gilbert, 2003; Moser et al., 2004; Singer and Clark, 1999).

Migration can also contribute to some pathological processes, including vascular disease, chronic inflammatory diseases, and tumour formation and metastasis. Thus, there is considerable interest in understanding cell migration on a molecular level because this could lead to novel therapeutic approaches, especially in areas of

biotechnology that focus on cellular transplantation and the manufacture of artificial tissues (Horwitz and Webb, 2003).

Beyond these physiological processes, cell migration is an important aspect of cancer metastasis where cancer cells exfoliate from the site of primary tumour formation and migrate to other organs within the body through the circulatory and lymphatic systems (Hanahan and Weinberg, 2000). Cell migration is inherently a multi-scale and multidisciplinary process that requires a thorough understanding of both the biochemical aspects of cell signalling and chemotaxis, and of the biophysical and mechanical aspects of cell-matrix interactions (Zaman et al., 2006).

There are a couple of types of cell movement that includes random movement (chemokinesis), directional migration (chemotaxis), and haptotaxis. Chemotaxis is the directed cell movement along a positive concentration gradient of chemoattractants, whereas haptotaxis is the cell motility in response to adhesive substrates such as extracellular matrix (ECM) (Rikitake and Takai, 2011). In general, cells become polarized in response to an extracellular stimulus that causes cells to move in a unidirectional manner. In the initial step of cell movement, actin-rich membrane protrusions such as filopodia and lamellipodia are extended and peripheral ruffles are formed at the leading edge in the direction of migration that results in the formation of an asymmetric cell front–rear polarity (Andrew and Insall, 2007; Arrieumerlou and Meyer, 2005; Dawe et al, 2003; Petrie, Doyle and Yamada, 2009). Under peripheral ruffles, focal complexes are formed and these immature cell–ECM adhesion structures are transformed into mature cell–ECM adhesion sites called focal adhesions during cell movement (Rikitake and Taiki, 2011).

Cell migration is a fundamental cellular process that involves the protrusion of the leading edge, the formation of new adhesive structures at the front, the contraction of the cell, and the release of adhesions at the rear (Rikitake and Taiki, 2011).

Today, we know that only a small portion of highly specialized cells is able to actively and autonomously migrate within the organism. These cells are: stem cells, leukocytes, fibroblasts, and tumour cells (Entschladen et al., 2005).

Typical cell migration assays are initiated by partial physical scraping of cell monolayers to mimic cell migration during *in vivo* wound healing (Sanghavi et al., 1994; Niea et al., 2007). Commonly, gradients of molecules were used in the body to regulate cell migration, axon extension, angiogenesis, and differentiation. Therefore, controlling

the spatial location of molecules on a surface or throughout a material could be potentially beneficial for tissue engineering (Kapur and Shoichet, 2004).

Hydrogels were synthesized with gradients of signalling or adhesive molecules or with varying crosslinking density across the material with the ability to direct cell behaviour such as migration, adhesion, and differentiation (Burdick, Khademhosseini and Langer, 2004; Zaari et al., 2004).

Migration is not limited to development, but occurs in the adult in both normal and pathological states. For example, skin is renewed continuously from precursors that migrate up from the basal layer. Migration also functions in the adult in immune surveillance, where leukocytes from the circulation migrate into the surrounding tissue to ingest bacteria. Tumour formation is accompanied by the invasion of blood vessels that arise from the proliferation and migration of their component endothelium. In metastatic cancer, some tumour cells acquire the ability to migrate out of the initial tumour into the circulation and move to new locations where they form a secondary tumour (Horwitz and Webb, 2003).

Recent evidence is pointing to plasticity in migration mechanisms. For example, the migration of cells *in vivo* differs from that of cells migrating *in vitro*. Migration *in vivo* is much more directed than that *in vitro* with cells forming long, stable protrusions pointed in the direction of migration. Tumour cells also show a plasticity that depends dramatically on the environment. Under some conditions they polarize and migrate along collagen bundles, whereas under others, they become more amoeboid and use different migration mechanisms (Horwitz and Webb, 2003).

Stem cells recently came into focus for migration studies, as researchers recognized that stem cells do not only reside in the tissue, e.g. the bone marrow, but actively migrate to certain areas of tissue regeneration such as the liver (Kollet et al., 2003; Masson et al., 2004).

2.2. Application of culture cells

Culture cells can be used in a diversity of applications, for example, in drug tests, chemical and biochemical assays.

2.2.1. Dimensional and tridimensional culture

Cells grow through interactions and communication with other cells within the living organisms that have complex and well-organized two-dimensional (2D) or three-

dimensional (3D) microscale systems composed of multilayers, membranes, protein channels, and many other elements (Yeon and Park, 2007).

Cells in their natural *in vivo* surroundings are exposed to a complex chemical and structural environment. The natural extracellular matrix is made up of structural components that are of nanoscale dimensions. Major fibrous extracellular molecules such as collagen fibers, elastin fibers, keratin fibers, and other have nanoscale diameters. It is highly important to mimic the natural environment when culture cells *in vitro* because cell behaviour is determined by both genetic make-up and the surrounding environmental cues. Cellular behaviours such as proliferation, differentiation, morphology, and migration are commonly controlled in culture by modulation of the chemical environment (Beachley and Wen, 2010).

Cell migration studies have focused primarily on migration in 2D environments, including a number of modeling endeavors (DiMilla, Barbee and Lauffenburger, 1991) over the past 20 years. Though these 2D analyses give us a fair insight on the mechanics of cell-substrate and cell-cell interactions, yet they still fall short of explaining the comprehensive *in vivo* processes due to lack of the 3D (Friedl and Brocker, 2000; Friedl and Wolf, 2003).

When cells migrate through 3D matrices they experience resistance through biophysical interactions with the visco-elastic matrix. This resistance is a unique feature of motility in 3D, as in the case of 2D motility, resistance is limited to interfacial 2D friction. In order to overcome this resistance the cells follow a sequence of adhesion and detachment events facilitated by the cell surface receptors (Friedl and Brocker, 2000; Wolf et al., 2003).

Fibrillar topographical cues in the form of 1D nanofibres can guide axonal growth and glial cell migration *in vivo* (Schnell et al., 2007; Tysseling-Mattiace et al., 2008). After spinal cord injury, the failure of axons to regenerate, results in paralysis. This clinical problem is due partially to the inability of axons to traverse scar tissue generated locally by glial cell infiltration into the wound that physically blocks axon regeneration (Tysseling-Mattiace et al., 2008). Immediately after a spinal cord injury in an animal model, introduction of peptide amphiphile molecules that self-assemble into nanofibres reduces glial scarring and promotes motor and sensory neuron outgrowth through the wounded region. While more investigation is required to understand how topographic physical cues are involved in directional migration *in vivo*, it is clear that association of cells with ECM with a defined structure, whether a 2D surface, a 3D

matrix, or a 1D line/nanofibre, can strongly affect cell polarity, cell morphology and cell migration (Petrie, Doyle and Yamada, 2009).

In vitro experiments show that parallel collagen fibres radiating outward from tumour explants can promote tumour epithelial cell invasion, while non-linear matrix reduces invasive behaviour (Provenzano et al., 2008). Tumour cells remodel the matrix into these parallel fibres in order to migrate. These data suggest that oriented ECMs play a role *in vivo* in directional migration and invasion. Understanding these mechanisms may provide better models for cancer metastasis and developmental processes (Petrie, Doyle and Yamada, 2009).

Recently, there has been increasing interest in culture in a 3D environment, predominantly in the areas of basic cell biology and drug testing. This is mainly because researchers are recognizing the limitations of 2D cultures, given the fact that they do not reproduce the morphology and biochemical features that the cells possess in the original tissue (Baharvand et al., 2006; Benya and Shaffer, 1982; Pardon et al., 2000).

It is well established that cells in a 2D culture environment physiologically differ from ones in a 3D architecture (Baharvand et al., 2006; Benya and Shaffer, 1982; Pardon et al., 2000). For example, articular chondrocytes lose their phenotypic characteristics in a 2D culture condition, whereas their biological functions are restored when the 2D cultured cells are transferred to a 3D environment (Benya and Shaffer, 1982). Consequently, it is of great interest to use 3D culture models, where cells are seeded in a 3D scaffold, to better mimic the *in vivo* conditions (Wu et al., 2008).

Many cell types, including tumour cells, chondrocytes, and embryonic stem cells, require a 3D microenvironment to properly demonstrate their *in vivo* physiology (Behravesh et al., 2005; Abbott, 2003; Birgersdotter, Sandberg and Ernberg, 2005; Camps et al., 2002; Cukierman et al., 2001; Levenberg et al., 2003; Martin et al., 2001; Mueller-Klieser, 1997).

2.3. Tumour cells lines

HeLa is an immortal cell line used in scientific research. It is the oldest and most commonly used human cell line, and it was derived from cervical cancer cells taken from Henrietta Lacks (Rahbari et al., 2009; Scherer, Syverton and Gey, 1953).

There are many different cell lines and some examples are shown in Table 1:

Table 1: Examples of some different human cell lines.

Human cell lines	Cell name	Description
Breast	MCF-7[1]	Human breast carcinoma cell line
Colon	COLO-205[1]	Human colon adenocarcinoma cell line
Skin	MEL-CLS-2[1]	Human skin melanoma cell line
Bone	HOS[1]	Human osteosarcoma cell line
Liver	HEP-G2[1]	Human hepatoma cell line
Leukemia	HL-60[1]	Human acute myelocytic leukemia (AML) cell line
Lung	NCI-H146[1]	Human lung small cell carcinoma cell line
	NCI-H460[2]	Human lung large cell carcinoma cell line
Stomach	AGS[1]	Human stomach adenocarcinoma cell line
Kidney	769-P[1]	Human kidney carcinoma cell line
Colon	HCT 116 (CCL-247)[2]	Human colorectal carcinoma
	HCT-15[3]	Human colon adenocarcinoma

The tumour cell lines have the advantage of being immortal. So, it is possible to replicate tumour cells indefinitely in time. Using mortal cell lines, the number of replications is limited to 50, which for drug tests may not be enough.

[1] http://www.cell-lines-service.de/content/index_eng.html
[2] http://www.lgcstandards-atcc.org/ ATCCCulturesandProducts/ CellBiology/CellLinesandHybridomas/tabid/981/Default.aspx
[3] http://www.hpacultures.org.uk/products/celllines/generalcell/

3. Blood Cells

The main constituents of blood are red blood cells (RBCs), white blood cells (WBCs), platelets and plasma. Plasma and RBCs are the biggest part of its constituents. RBCs or erythrocytes do not have nuclei and their main function is oxygen transport. WBCs or leukocytes have nuclei and subdivide in lymphocytes, granulocytes and macrophages. Leukocytes are the first immune response of our organism. Platelets or thrombocytes do not have nuclei and their function is the close of ruptures in vascular walls. At last, plasma is composed mostly with water, sugars and proteins. Its function is carrier nutrients, RBCs, white cells and platelets.

In microcirculation, which comprises the smallest arteries and veins, the flow behaviour of individual blood cells and their interactions provide the microrheological basis of flow properties of blood at a macroscopic level. As a result, in microcirculation it is fundamental to study the flow behaviour of blood at cellular level. Thus, blood is not a homogeneous fluid, but one composed by a suspension of cells, proteins and ions in plasma. In normal blood, three types of cells comprise about 46% of its volume. These cells are RBCs representing 45% of volume, WBCs and platelets (Figure 2) (Garcia, Dias and Lima, 2012).

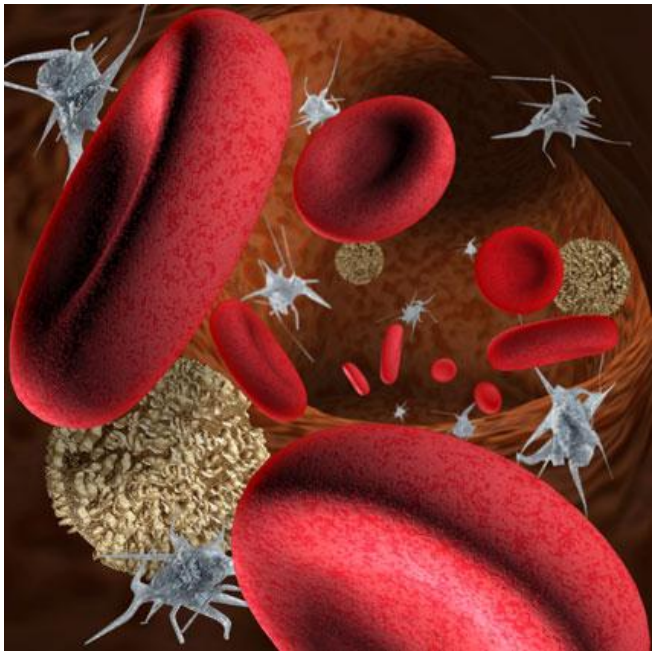

Figure 2: Red blood cells, white blood cells and platelets (adapted of Discover Magazine).

3.1. Erythrocytes deformation

RBC deformability is the ability of RBC to deform under applied stresses, which is important for the delivery of oxygen to tissues. *In vitro* blood flow behaviour in microchannels is strongly influenced by the RBCs, since they occupy almost half of whole blood volume (Lima et al., 2012). Important factors that determine RBC deformability include the cell volume to surface area ratio, the viscosity of the cytoplasm, and the elastic behaviour of its membrane (Mohandas and Chasis, 1993; Mohandas and Evans, 1994). RBCs are formed in the bone marrow and during maturation they lose their nuclei before entering the circulatory system. When suspended in an isotonic medium, RBCs have a biconcave discoid shape, with a major diameter of about 8 μm. The density of a RBC is about 1.08×10^3 $kg.m^{-3}$ and its major cellular components are the cytoplasm and a thin membrane composed of lipid bilayer and protein molecules that together determine its elastic properties (Evans, 1973; Evans and La Celle, 1975; Lima et al., 2012). There is experimental evidence that healthy RBCs are extremely deformable into a variety of shapes in flowing blood in response to hydrodynamic stresses acting on them (Lima et al., 2012). The RBCs elongate significantly when they pass through capillaries, the diameter of which is smaller than the diameter of RBCs at rest (Caro et al., 1978; Hardeman and Ince, 1999).

Early studies of micropipette aspiration of the RBC have already indicated the crucial role that membrane shear deformation plays in RBC deformability (Evans 1973; Evans and La Celle 1975). These analyses were performed under the assumption that the skeleton is incompressible. However, Discher et al. (1994), using fluorescence to image the deformation of the skeleton, demonstrated that the skeletal density of the pipette-aspirated membrane is non-uniform. Based on this evidence, Mohandas and Evans (1994) and Boey et al. (1998) developed elastic constitutive models of the membrane that account for the skeleton area expansion.

The deformability can have serious consequences leading to health problems (Cho, Mooney and Cho, 2008). In fact, it has been suggested to certain diseases and therefore determination of RBC deformability may be an important tool in medical diagnosis (Hardeman and Ince, 1999; Hou, et al., 2010; Tsukadaet al., 2001).

So far, many investigations on human RBC deformability have been performed using a variety of techniques, including optical tweezers and micropipeting (Musielak, 2009; Shin et al., 2007).

Important studies in biomicrofluidics devoted to blood rheology and its flow dynamics in microchannels, which have played a key role in several recent developments of lab-on-chip devices for blood sampling, analysis, and cell culture (Abkarian, et al., 2008; Chau, Rolfe and Cooper-White, 2011; Faivre et al., 2006; Fujiwara, et al., 2009; Nakano, et al., 2010).

Researchers, such as Shevkoplyas et al. (2005, 2006) Yang et al. (2006) and Faivre et al. (2006) took advantage of the natural flow properties of blood in microcirculation, such as plasma skimming, leukocyte marginalization, the bifurcation law, and cell-free layer enhancement by an abrupt constriction, to design microfluidic devices to separate plasma and leukocytes from the whole blood.

The complexity of controlling and obtaining detailed measurements of the blood flow behaviour through *in vivo* microvascular systems (Nakano et al., 2005) has led to *in vitro* studies being performed by using polydimethylsiloxane (PDMS) microchannels obtained by means of a soft-lithography technique (Ishikawa, et al., 2011; Lima, et al., 2011; Shevkoplyas et al., 2005; Shevkoplyas et al., 2006;).

4. Microfabrication

Microfabrication such as micromachining, micromanufacturing or micro eletromechanical system (MEMS) is a technique used in fabrication of devices with very small dimensions in the micrometer range (Madou, 2002). Soft lithography is a set of microfabrication techniques that use elastomeric stamps fabricated from patterned silicon wafers to print or mould materials at resolutions as low as several hundred nanometers (Kane et al., 1999; Ostuni et al., 2001; Ostuni, Yan and Whitesides, 1999; Xia and Whitesides, 1998A).

In the past few years, microfabrication has been increasingly used in biomedical, biochemical and biological applications, for both fundamental research and device application, altogether called BioMEMS (Madou, 2002; Whitesides et al., 2001; Ziaie et al., 2004).

Principal advantages to use the BioMEMS techniques are (Duffy et al., 1998; Madou, 2002;Ziaie et al., 2004;):

a) Obtain small dimensions with high resolution and sensitivity;
b) Ability to incorporate sensing and actuating functions in proximity or on the same substrate;
c) Ability to incorporate, probe, manipulate, and study molecules and cells;
d) Minimal invasiveness;
e) Portability;
f) Shorter analysis time; and
g) Ability to facilitate high-throughput experimentations due to redundancy and arrays.

Microtechnology can facilitate the study of cell behaviour *in vitro* because it provides the necessary tools for recreating *in vivo*-like microenvironments (Walker et al., 2004). Therefore, microfluidic devices for cell culture studies are rapidly gaining importance in drug development and biological research applications, such as drug toxicity or metabolism studies, and stem cell differentiation studies (Toh et al., 2007).

Microfabrication is separate in two categories: hard micromachining (using hard materials like silicon, glass and metal) and soft micromachining (using soft material like

polymer and gels) (Ziaie et al., 2004). The most important steps used by the two categories are shown in Table 2.

Table 2: Steps of hard and soft micromachining (Campbell, 2001; Jaeger, 2002; Xia and Whitesides, 1998A; Ziaie et al., 2004)

Hard micromachining	**Soft micromachining or soft lithography**
Thin film deposition	Micromolding
Lithography	Hot embossing
Etching	Microcontact printing
Substrate bonding	

4.1. Photolithography

Photolithography has some typical steps (Li, Tourovskaia and Folch, 2003; Wen, 2009):

a) 2D pattern is first created with a computer-aided design software;
b) Photomask is then generated following the CAD design;
c) After thin-film deposition of the desired material on a silicon wafer, a thin and uniform layer of photoresist is spin coated, Figure 3A;
d) Coated wafer is soft baked, removing the solvents and enhancing adhesion;
e) Wafer is exposed to UV (ultraviolet) light under the photomask, Figure 3B;
f) Unpolymerized photoresist is dissolved off the wafer;
g) Hard bake is used to further improve the adhesion and concludes the process.

The process is basically as shown in Figure 3.

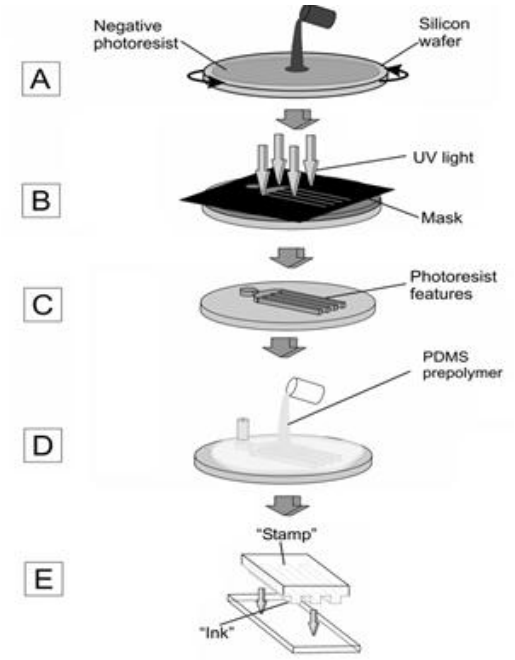

Figure 3: General process flow in photolithography (adapted from Li, Tourovskaia and Folch, 2003).

An important lithography step is the photoresist. The composition of a photoresist is a polymer (base resin which changes structure upon radiation), a sensitizer (controlling the photochemical reactions in the polymer), and a casting solvent (allowing thin layer formation by spin coating). There are two types of photoresist in response to UV exposure. One is called positive tone (for example PMMA), (Madou, 2002). The most common negative photoresist is SU-8 epoxy, invented by IBM scientists. SU-8 is composed of EPON SU-8 resin and a photosensitizer triaryl sulfonium salt (Angelo et al., 1992; Lee et al., 1995). SU-8 resist is specifically designed for micromachining for thick films up to 500 μm in a single coat and has excellent sensitivity, high resolution, low optical absorption, high aspect ratios, and good thermal and chemical stability, with low cost (Bertsch, Lorenz, Renaud, 1999; Madou, 2002).

Spin coating is achieved by dispensing a viscous solution of resist onto the wafer placed on a vacuum chuck. Then the wafer is spun at a high speed, ranging from 1500 to 8000 rpm, depending on the viscosity and the desired thickness, to form a uniform film of photoresist. This is a critical step to ensure the success of pattern transfer, which should be done with extreme care to eliminate defects and ensure uniformity. After spin coating, a soft baking ensues at 75 to 100 ºC for, say, 20 min to evaporate the solvent and to remove the built-in stress, in order to enhance the adhesion of the resist to the silicon wafer (Wen, 2009).

The unpolymerized photoresist needs to be washed away from the wafer, leaving the desired latent features to stand out, which may be used as a mask for further subtractive or additive steps or as a mold for pattern transfer with soft lithography. There are two major technologies for development: wet development and dry development. The first is widely used in microfabricatioin in general, and the latter is beginning to substitute wet development for applications with fine line width resolution. Dry development is devised to overcome some disadvantages of wet development, such as some swelling of the resist in organic solvents and loss of adhesion. However, dry developed resists should be used (Madou, 2002).

Soft materials, such as polymers and gels, are amenable to a series of micromolding techniques under relatively mild conditions, such as replica molding (REM), microtransfer molding (μTM), micromolding in capillaries (MIMIC), and solvent-assisted micromolding (SAMIM), Figure 4 (Wen, 2009).

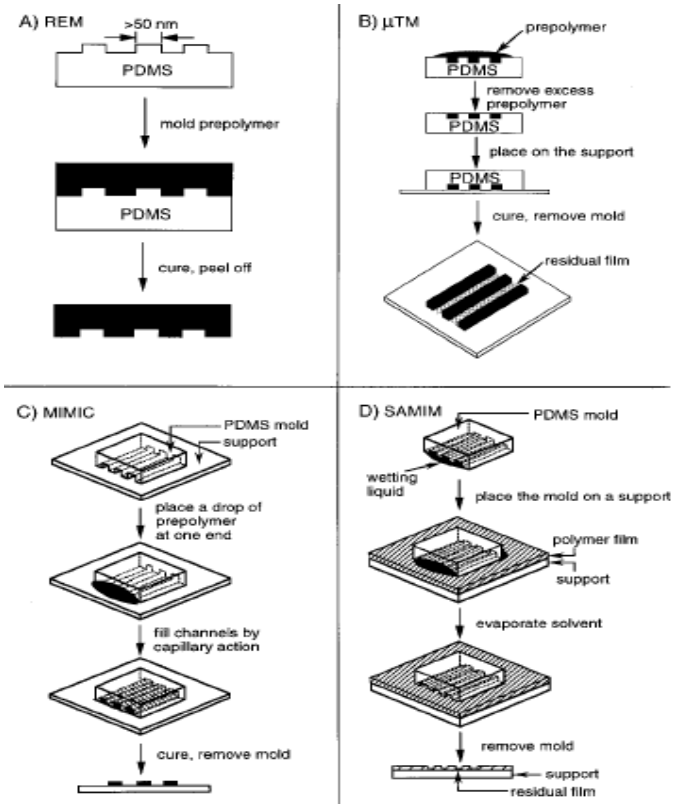

Figure 4: Schematic illustration of micromolding techniques. A) replica molding, B) microtransfer molding, C) micromolding in capillaries, and D) solvent-assisted micromolding (Xia and Whitesides, 1998A).

Replica molding duplicates the shape, the morphology, and the structure from a master. It has the capability of 3D pattern transfer in one step, whereas photolithography does not have this capability. The process is reliable, fast, simple and inexpensive with a

resolution as small as below 100 nm for which photolithography runs to its limit due to optical diffraction (Madou, 2002; Xia and Whitesides, 1998A).

In μTM, a drop of prepolymer is applied on the surface of an elastic master and the excess liquid is removed, which is followed by placing it against a substrate. After the prepolymer is cured and the master is removed, a patterned microstructure is left on the surface of the substrate (Zhao, Xia and Walker, 1996). Both isolated and interconnected microstructures may be obtained through μTM with the advantage over other microfabrication techniques that microstructures may be transferred to nonplanar surfaces, which facilitates the fabrication of multiple layers of 3D structures (Xia and Whitesides, 1998A).

In MIMIC elastomeric master is placed in conformal contact with the substrate, leaving the interconnected microfeatures to form a network. Then a low-viscosity pre-polymer is applied at the open ends of the network and sipped in by capillary force. After curing of the precursor and the removal of the master, an interconnected microstructure may be formed on the substrate surface. MIMIC is a convenient microfabrication technique (Xia and Whitesides, 1998A).

SAMIM shares some characteristics of replica mold and embossing. In SAMIM, an elastomeric master is wetted with a solvent that well dissolves the substrate polymer but not the master, and brought into contact with the substrate. The solvent swells a thin layer of the polymer, in which the microstructures may be generated according to the master's topology. The success of SAMIM depends on the choice of the solvent, which not only should have selectivity in dissolution but also should have high gas pressure. The SAMIM procedure is a simple technique to form complex quasi-3D features in one step. It is different from commonly used hot embossing, in that it uses solvent to soften the polymer substrate instead of heat, and the master is elastomer instead of hard materials (Xia and Whitesides, 1998A).

Both techniques (hard and soft micromachining) need a clean room to do some processes, because this is sensitive procedures and all carefully are necessary. Table 3 presents the classifications of clean rooms.

Table 3: Clean room classifications (adapted of Data Recovery).

Class	Maximum number of particles per cubic foot of air of diameter greater than or equal to each indicated size					Typical uses
	0.1 µm	0.2 µm	0.3 µm	0.5 µm	5.0 µm	
1	35	7.5	3	1	—	integrated circuits
10	350	75	30	10	—	manufacturing
100	—	7502	300	100	—	hard drive manufacturing hard drive data recovery miniature ball bearings assembly photo labs medical implants
1000	—	—	—	1000	7	pharmaceutical manufacturing
10000	—	—	—	10000	70	colour TV tubes hospital operating room
100000	—	—	—	100000	700	ball bearings

4.2. PDMS

PDMS is a silicone elastomer and has been the most popular soft material in biomedical microfabrication applications due to very suitable physical and chemical properties, Table 4 (Makamba, et al. 2003; McDonald and Whitesides, 2002; Toepke and Beebe, 2006).

Table 4: Physical and chemical properties of PDMS (Adapted from McDonald and Whitesides, 2002).

Property	Characteristic	Consequence
Optical	Transparent; UV cut off, 240nm.	Optical detection from 240 to 1100 nm.
Electrical	Insulating: breakdown voltage, 2e7V/m	Allows embedded circuits; Intentional breakdown to open connections.
Mechanical	Elastomeric; tunable Young's modulus, typical value of ~750kPa	Conforms to surfaces; allows actuation by reversible deformation; Facilitates release from moulds.
Thermal	Insulating; thermal conductivity 0.2W/(m.K); coefficient of thermal expansion, 310μm/(m.ºC)	Can be used to insulate heated solutions; does not allow dissipation of resistive heating from electrophoretic separation
Interfacial	Low surface free energy ~20 erg/cm2 contact angle of Sylgard-184: ~110º	Replicas release easily from moulds; can be reversibly sealed to materials
Permeability	Impermeable to liquid water; permeable to gases and nonpolar organic solvents; oxygen diffusion coefficient 3.55×10-5 cm2/s	Contains aqueous solutions in channels; allow gas transport through the bulk material; incompatible with many organic solvents
Reactivity	Inert; can be oxidized by exposure to a plasma; Bu4N+F-((TBA)F)	Unreactive toward most reagents; surface can be etched; can be modified to be hydrophilic and also reactive toward silanes; etching with (TBA)F can alter topography of surfaces
Toxicity	Nontoxic	can be implanted *in vivo*; supports mammalian cell growth

The porous nature of PDMS is convenient for cell-based studies, because it allows oxygen and carbon dioxide to freely diffuse through it (Makamba et al., 2003; Toepke and Beebe, 2006).

PDMS has been the most popular material in microfluidics community as it is optically transparent, chemically inert, biologically compatible, inexpensive and easy to pattern by soft lithography (Li, Tourovskaia and Folch, 2003; Makamba, et al. 2003; Toepke and Beebe, 2006). These properties may be translated to the following important operation advantages:

a) PDMS has high fidelity in pattern transfer down to 10's of nm (McDonald and Whitesides, 2002);
b) It is an elastomer which has superior conformability to other surfaces and may be actuated for making microfluidic components, such as pumps and valves (Berg et al., 2003; Grover et al., 2006; Thorsen, Maerkl and Quake, 2002);
c) It has good sealing with itself and other surfaces, both reversibly and irreversibly, such as silicon, glass, polystyrene, polyethylene, or silicon nitride, provided both the surfaces are treated with oxygen or air plasma for about one minute (Chaudhury and Whitesides, 1991; Li, Tourovskaia and Folch, 2003; McDonald et al., 2000) or exposed to UV/ozone (Efimenko, Wallace, and Genzer, 2002), for irreversible sealing;
d) PDMS may form complex 3D networks by stacking multiple layers in alignment due to its transparency and good sealing (Anderson et al., 2000);
e) PDMS is highly permeable to gases, especially nonpolar gases, such as O_2, N_2 and CO_2 (Charati and Stern, 1998; Erdodi and Kennedy, 2005; Whitesides et al., 2001), which facilitates cell-based applications.

However, PDMS is hydrophobic, which may constitute some challenges in microfluidic applications due to capillary pressure (Whitesides et al., 2001). But the surface of PDMS may be rendered hydrophilic by strong oxidants, such as oxygen plasma or UV/ozone, with comparably limited degrees, but may recover to hydrophobic in a few minutes in the air. Storage in water may slow the recovery process. In addition, PDMS is prone to protein adsorption and biofouling (Wen, 2009).

The most widely used PDMS is Sylgard 184 silicone elastomer kit from Dow Corning, composed of a base and curing agent. When forming the elastomer, the liquid prepolymer base and the catalytic curing agent is mixed by a ratio of about 10:1 and heated to about 70ºC for 2 hours (Wen, 2009).

One of the major drawbacks of PDMS film is that its surface is highly hydrophobic in nature with very low surface energy (Morent et al., 2007) which greatly impedes its usage without undergoing appropriate surface modification. This property of PDMS poses serious problem in various applications like reliable PDMS–PDMS bonding (Bhattacharya et al., 2005) in microvalves and micropumps (Jeon et al., 2002; Yang and Lin, 2007), fluid flow through microfluidic channels in electrokinetic applications (Vickers, Caulum and Henry, 2006), attachment of animal cells for cell

culture (Wu, 2009), deposition of metal thin films for realization of microelectrodes and microcircuit connections in flexible electronics (Axisa et al., 2007; Lacour, Tsay and Wagner, 2004; Morent et al., 2007). Thus, it is important to modify the PDMS surface for successful realization of such microdevices.

A variety of solutions, primarily surface modifications, have been proposed, for example, oxygen plasma treatment, silanization, adsorbed coatings (Polybrene/dextran sulfate), and protein or lipid coatings (Duffy et al., 1998; Barker et al., 2000; Grzybowski et al., 1998; Linder et al., 2001; Liu, et al., 2000). However, surface modifications such as oxygen plasma treatment and adsorbed coatings can be unstable requiring periodic reapplication.

Protein-based coatings frequently result in ill-defined and heterogeneous surface properties as proteins are attached in a multiplicity of orientations with some molecules denatured and others folded (Hu et al., 2002).

Some hybrid microdevices (i.e. PDMS/glass) were also fabricated, e.g. a microsystem dedicated for growing and monitoring of cell lines and testing their exposure to drug or toxin (Hung et al., 2004; Prokop et al., 2004).

4.2.1. Surface modification of PDMS

Surface modification techniques include the dry method: activation of PDMS surface with air/oxygen/argon, UV/Ozone and corona discharge technique. The wet method includes: deposition of a suitable layer over the PDMS surface through physical adsorption of charged amphiphilic molecules, copolymer layer, layer-by-layer (LBL) self-assembly or through chemical modification using self-assembled monolayers (SAM), UV grafting or direct treatment with reactive chemicals like piranha solution (Maji, 2012).

Maji, Lahiri and Das (2012) studied the hydrophilicity of PDMS using the piranha and potassium hydroxide (KOH) with good results for time treatment equal 15 minutes where the measured of contact water was 27º.

PDMS is hydrophobic and this characteristic has a crucial importance when we work with cells, because cells are almost water. So, the PDMS repels the cell and it is not possible the attachment and proliferation in this conditions.

For this problem, some researchers choose different techniques like oxygen plasma, UV-grafting, piranha and KOH solution.

The methods for surface modification can be divide in two categories, the dry methods that include air/oxygen/argon plasma, UV/Ozone and corona discharge technique, and the wet methods, that include deposition od a suitable layer, copolymer layer, layer-by-layer (LBL) self-assembly and chemical modifications like SAM, UV-grafting (Hu et al., 2002) and piranha solution (Maji, Lahari and Das, 2011).

Oxygen plasma is the option of most researchers, but have more cost comparative with others. For example the piranha solution has a low cost and this preparation is very simple and results are in the majority of cases the same as oxygen plasma.

4.2.1.1. Adhere microdevices on different substrates

Building a microfluidic device presents some challenges. Sometimes is difficult the union of the device to a substrate; it is necessary to pay attention which materials are used. In this case the main materials of microdevices and substrates are PDMS/glass and PDMS/PDMS, because it is necessary a clear view for the cell observation. Depending of the device objective two options exist: reversible bonding or irreversible bonding.

The irreversible bonding is a definitive attach of the materials and methods like oxygen plasma or UV/ozone were used (Efimenko, Wallace and Genzer, 2002). These methods affect the surface properties of the substrates.

The irreversible bonding is a non-definitive attach of the materials. Some researchers like Wen use a technique of reversible packing which is a method of frame-assisted assembly (FAA), Figure 5.

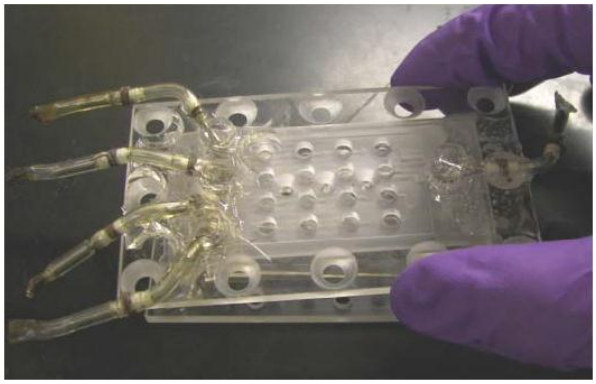

Figure 5: Reversible packing with wholes to insert the screws and inlets for the microfluidic device (adapted from Wen, 2009).

Liu et al. (2009) tried another strategy to sealing the device with scotch tape. In this case, it was possible to use the mentioned method because their project did not

involve cells. Their device was for immunoassays and used proteins. The tape could be toxic for cells and kill them.

4.3. Microfluidics

With the help of recent advances in microfluidic technology, a cell culture system can be miniaturized into a microfluidic device, which can largely minimize the chemical gradient phenomena existing in culture environments and cultured constructs and hence provides better control over the cells' microenvironments (Wu et al., 2006). It also reduces the number of cells required and the need for large volumes of culture medium and costly reagents.

Microfluidic systems have been developed by several groups to attempt to create microenvironments of greater physiological relevance and high-throughput platforms for cell behaviour analysis (Walker, Zeringue and Beebe, 2004).

While traditional non-microfluidic (static) cultures can be straightforwardly maintained by occasional medium replacements, microfluidic cultures cannot be treated as static because the average volume of medium per cell is typically one order of magnitude smaller than in macroscopic cultures (Tourovskaia, Figueroa-Masot and Albert Folch, 2004), Figure 6.

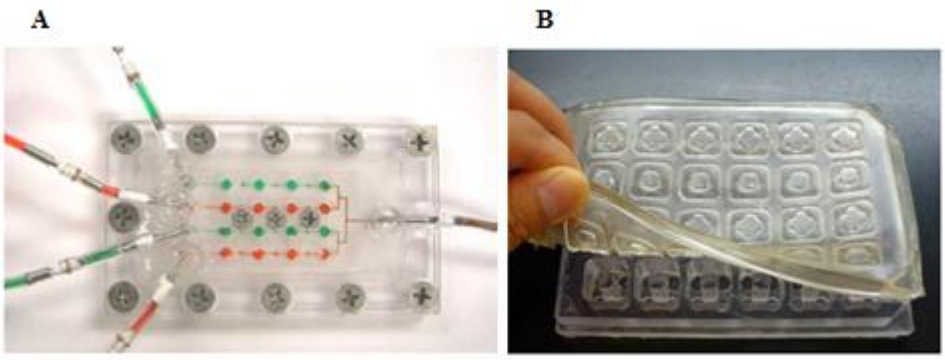

Figure 6: Two different culture cells. A – Microfluidic culture with dynamic flux; B – Microplate for culture with PDMS to seal the top (Wen, 2009).

Miniaturization has started to play an important role in genomics and proteomics, clinical diagnostic in medical sciences, pharmacology, tissue engineering and cell biology (Khademhosseini et al., 2005).

Microfluidic chambers enable spatial and temporal control of solubilized factors such as oxygen and nutrients, allowing for a more realistic replication of the complex conditions found *in vivo* than in conventional cell-culture set-ups (Hu, Quaranta and Li, 2007).

The typical microfluidic channel has a minimum dimension on the scale of 1 to 1,000 μm. A standard microfluidic network may consist of a set of 10 interconnected channels, each 100 μm in height and width, and 10 mm in length, giving a total fluid volume of 1 μl. On this scale, it is important to consider the fluid mechanics and mass transport differences in comparison with a standard culture dish (a 60 mm culture dish has no flow, and roughly 4,000 μl of volume) (Lee, Gaige and Hung, 2011).

In addition, micro scale technologies allow for an unprecedented ability to control the cellular microenvironment in culture and miniaturize assays for high-throughput applications (Khademhosseini et al., 2005).

4.3.1. Microfabricated device for cells

Microfabricated devices create unprecedented opportunities to study and utilize biological cells (El-Ali, Sorger and Jensen, 2006), with unique advantages of highly tailor able microenvironment that is of cellular relevant dimensions (from nm to μm) and of highly parallel experimentation that may generate abundant information. Therefore, the techniques for culturing, stimulation, handling, and analysis for cells at microscale have made tremendous progress since their combination, making microscale systematic cell-based studies possible, but still with substantial challenges in fabrication, integration and packaging (Wen, 2009).

Cells are fragile and sensitive, and their good maintaining and growth are usually the starting point for further experiments. Microfabricated devices for cell culture, cell monitoring and cell-based assay have tremendous advantages with high-throughput and high-content capabilities. There are three major driving forces for developing such systems: tissue engineering, cell-based assays, and bioprocess parameter characterization (Wen, 2009).

5. Tissue Engineering

The term "tissue engineering" has emerged at a meeting sponsored by the National Science Foundation (NSF) in 1987. Other definitions exist: Langer and Vacanti (1993) defined tissue engineering as "an interdisciplinary field that applies the principles of engineering and the life sciences toward the development of biological substitutes that restore, maintain or improve tissue function." Galletti, Hellman, and Nerem (1995) defined tissue engineering as "the basic science and development of biological substitutes for implantation into the body or the fostering of tissue remodelling for the purpose of replacing, repairing, regenerating, reconstructing, or enhancing function." These subsequent definitions essentially reiterate the NSF definition. Two other recently popular terms, regenerative medicine and reparative biology, have considerable, sometimes total, overlap with the aims and goals of tissue engineering.

Tissue engineering has emerged as an attempt to resolve the short age in tissues and organs for transplantation therapy, by developing tools for biological substitutes that would repair and replace damaged tissues and organs in the body (Cima et al., 1991; Khademhosseini et al., 2005; Langer and Vacanti, 1993; Nerem, 1991).

One of the major challenges for tissue engineering is to create a favourable environment for the proliferation and differentiation of cells into functioning tissues. Three main elements compose engineered tissue, namely the scaffold, the cells and the environment in which the cell-scaffold constructs are cultured and conditioned. The design and function of synthetic scaffolds can be optimized, allowing for control of cell behaviour following seeding onto a final product. Numerous scaffold properties can be manipulated, including the type of material utilized, the shape and size of pores in which cells are located, the mechanical integrity of the construction, substrate coating aimed towards promotion of cell adhesion and incorporation of chemicals and growth factors conducive to optimized tissue formation and function (El Haj et al., 2005).

In general, there are three main approaches to tissue engineering: (i) to use isolated cells or cell substitutes as cellular replacement parts, (ii) to use a cellular biomaterials capable of inducing tissue regeneration, and (iii) to use a combination of cells and materials (typically in the form of scaffolds) (Griffith and Naughton, 2002).

Figure 7 shows the various approaches in tissue engineering using cells, scaffolds, or their combination.

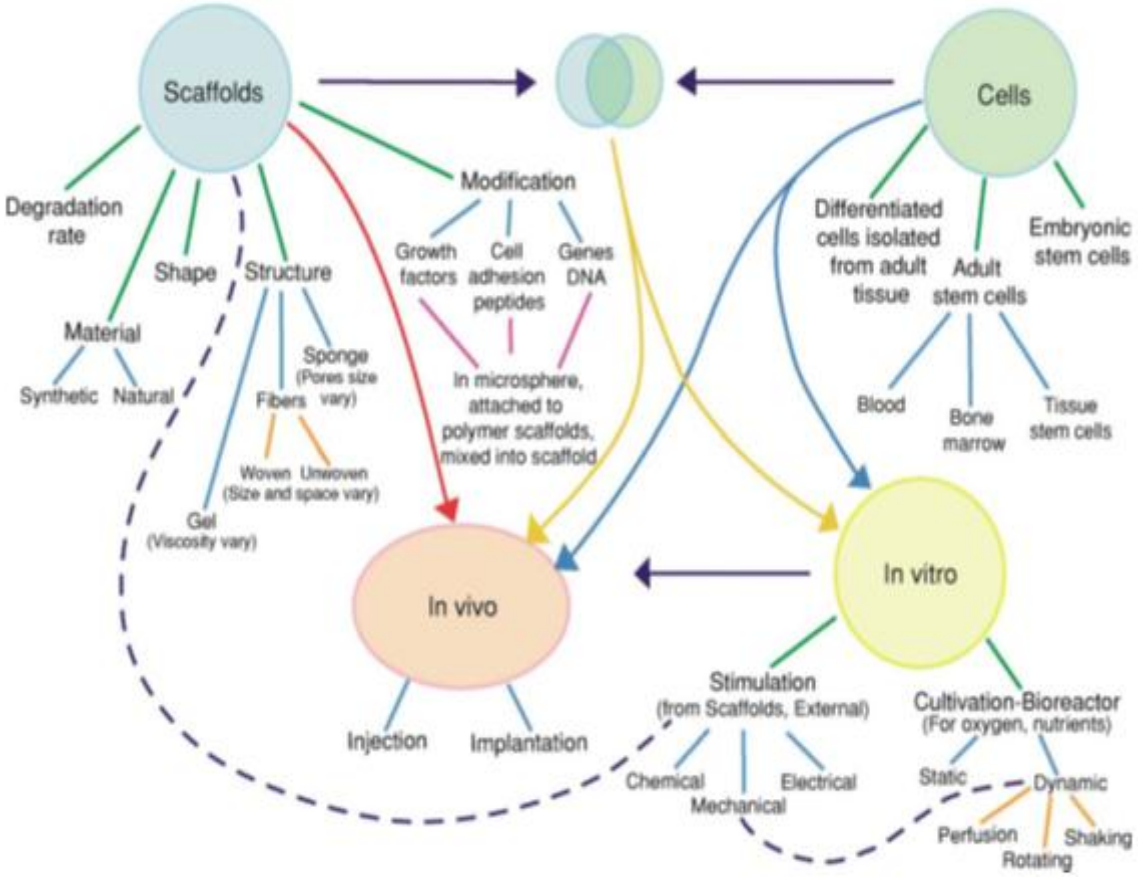

Figure 7: Diagram showing the various approaches in tissue engineering using cells, scaffolds, or their combination (Levenberg and Langer, 2004).

Generally, it is considered that there is a triad of key factors on tissue engineering (Lanza, Langer and Vacanti, 2000), which are cells, tissue-inducing substances and scaffolds. Following this line, another critical factor, bioreactors, is counted in to make this group a quartet (Wen, 2009).

5.1. Cells

Recently, there has been increasing interest in culturing in a 3D environment, predominantly in the areas of basic cell biology and drug testing. This is mainly because researchers are recognizing the limitations of 2D cultures, given the fact that they do not reproduce the morphology and biochemical features that the cells possess in the original tissue (Baharvand et al., 2006; Pardon et al., 2000).

Cells are placed on or within porous matrices, which could be naturally originated, such as collagen and fibrin, or synthetic, such as polymers. For synthetic polymer scaffold materials, it has been found that the bulk material, 3D morphology, structure, porosity, surface chemistry and mechanical properties of scaffolds need to be specifically designed and processed to facilitate cell proliferation, migration and function (Griffith, 2000; Muschler, Nakamoto and Griffith, 2004). The methods for fabricating porous scaffolds include particulate leaching, freeze-drying, gas infusion, and phase separation, etc, which generally create isotropic microstructures (Muschler, Nakamoto and Griffith, 2004; Yang et al., 2001). There are also novel techniques to make scaffolds with designed microstructures, such as solid-free-form fabrication methods (e.g. three-dimensional printing process and stereolithography) (Griffith and Naughton, 2002; Landers et al., 2002) and multi-layer scaffolds with well-defined dimensions using microembossing and carbon dioxide bonding (Yang et al., 2005).

When cells are not directly incorporated into a nanofiber scaffold, the scaffold may be populated by cells that migrate into the interior of the scaffold from the outer surface. The extent of cell migration into nanofiber scaffolds can be affected by both the architecture of the scaffolds and the biological or chemical cues incorporated into the scaffold (Beachley and Wen, 2009).

Cell migration is a critical process in determining the success of tissue regeneration. In many designs, tissue scaffolds are populated by cells due to cell migration, either from cells seeded on the scaffold surface *in vitro* or endogenous cell migration *in vivo*. Tissue engineering scaffolds designed with controlled conduction of cell migration are desirable, and nanofibrous architecture can have a significant effect on cell migration properties *in vitro* and *in vivo* (Beachley and Wen, 2010).

For cell migration into a nanofibrous scaffold occur there must be adequate void space for cells to occupy and move around. In the case of randomly aligned electrospun mats, pore size is generally related to fiber diameter, where scaffolds fabricated from larger fibers have larger pores and thus greater permeability to cell infiltration (Eichhorn and Sampson, 2005). Optimal pore size may be dependent on the specific cell type or application, but the minimum pore size necessary for infiltration must not be significantly smaller than that of the migrating cells. The trade-off between scaffold porosity and fiber diameter in electrospun scaffolds is one of the current limiting factors of this technology in tissue engineering (Beachley and Wen, 2009).

For cell-based tissue engineering, isolated cells are the raw material. So far virtually every mammalian tissue has been attempted to be tissue engineered (Langer and Vacanti, 1993). The sources of cells may include autologous cells from the patient, allogeneic cells from a human donor, and xenogeneic cells from a different species. Each category may also be divided as adult cells or embryonic stem (ES) cells. However, the cell sources impose the number one challenge for tissue engineering due to the lack of proper cells (Griffith and Naughton, 2002), though there have already been skin substitutes developed for successful healing surgeries (Mansbridge et al.,1998). There have been high hopes for ES cells, but the source for ES cells itself is a controversial problem and possible immunological barriers are not fully explored (Griffith and Naughton, 2002). However, adult stem cells, such as bone-marrow stem cells and haematopoietic stem cells, or applied together with ex vivo gene therapy techniques, have shown huge potentials for various tissue regenerations (Bianco and Robey, 2001).

5.1.1. ADSCs

ADSCs have a great potential for use in tissue repair and regeneration in the field of plastic and reconstructive surgery. Although the current applied strategies for adipose tissue engineering have advanced in the past years, complete understanding of the mechanisms of interactions among adipose stem cells, growth factors and biomaterials in tissue engineering is needed to advance the end goal of developing 'off-the-shelf' tissue-engineering products. The enthusiasm over what unquestionably represents a markedly innovative technique with huge therapeutic potential must be balanced, although against stringent standards of scientific and clinical investigation, before this new technology has its applications (Sterodimas et al., 2010).

Stem cells, like ADSCs, because of their pluripotentiality, proliferative efficiency, low donor morbinidity and unlimited capacity for self-renewal, project great promise for tissue engineering and are expected to allow significant advances for distinct reconstructive procedures (Ogawa, 2006; Sterodimas et al., 2010).

Chemical composition, mechanical stability and 3D architecture of the scaffold are crucial factors for tissue engineering with ADSCs. Cellular penetration, sufficient proliferation and full differentiation inside the construct after transplantation must be guaranteed (Hemmrich and von Heimburg, 2006). The limited materials that are currently available as carriers or scaffolds in the field of plastic and reconstructive

surgery necessitate the introduction of innovative ‘smart’ materials that will control tissue topology and have surface modifications to stimulate cell attachment, differentiation and growth (Sterodimas et al., 2010).

5.2. Nanofibers scaffolds

Most nanofibers obtained so far are in non-woven form, which can be useful for relatively small number of applications such as filtration (Gibson, Schreuder-Gibson and Riven, 1999), tissue scaffolds (Fertala, Han and Ko, 2001), implant coating film (Buchko et al., 1999), and wound dressing (Jin et al., 2002).

When the diameters of polymer fiber materials are shrunk from to submicrons or nanometers, there appear several amazing characteristics such as very large surface area to volume ratio (this ratio for a nanofiber can be as large as 103 times of that of a microfiber), flexibility in surface functionalities, and superior mechanical performance (e.g. stiffness and tensile strength) compared with any other known form of the material (Huang et al., 2003).

Many different applications for nanofibers in tissue engineering have been explored. Because polymer nanofibers can provide 3D architecture, modulate cell behaviour, and have the potential to deliver biomolecules, they are a good candidate for a wide variety of tissue engineering applications. Table 5 shows some types of tissue and how nanofibers can be applied (Beachley and Wen, 2009).

Table 5: Nanofibrous scaffolds for tissue engineering applications (adapted of Beachley and Wen, 2009).

Tissue Type	Promotion of desired behaviours from tissue specific cells *in vitro*	Favorable Structural properties for tissue specific application	*In vivo* models
Bone	Osteoblastic and pre-osteoblastic cells Mesenchymal stem cells	Selective pore size	Subcutaneous implantation Bone Defect-Skull Bone defect- Femur
Vascular	Endothelial cells Smooth muscle & endothelial cells	Shape & mechanical properties	Epigastric vein graft Abdominal aortic graft
Neural	Brain derived neural stem cells Dorsal root ganglion (DRG) DRG & perineural membrane derived primary neurons	Shape	Severed optic tract Spinal cord transaction Tubular sciatic nerve bridging device

In addition to the structural roles of nanofibers, they may also elicit functional responses in cells to migratory and remodelling behaviours. Nanofibrous structure induced fibroblasts to increase production of collagenase that degrades the adhesive collagen between the scaffold surface and cell membrane, and this lead to the hypothesis that the nanofibrous architecture may have been encouraging migratory or remodelling behaviour in comparison to a smooth surface (Meng et al., 2009).

A wide variety of biodegradable and biocompatible polymers have been processed to fabricate stereoregulated scaffolds, including synthetic polymers, such as poly(lactide) (PLA), poly(glycolide) (PGA) and their copolymers poly(lactide-co-glycolide) (PLGA), poly(ε-caprolactone) (PCL), and natural polymers, such as collagen, protein, and fibrinogen (Langer and Tirrell, 2004; Malafaya, Silva and Reis, 2007; Sokolsky-Papkov et al., 2007). Table 6 shows some materials with relevant features and applications.

Table 6: Materials for tissue engineering scaffolds.

Material		Relevant features and application
Naturally-derived	Collagen-based scaffolds	Soft tissue repair, Cell differentiation, Capillary engineering, Dermis engineering, Vascularized adipose tissue (Battista, et al., 2005; Hudon, et al., 2003; Pachence, 1996; Stark, et al., 2006; Sokolsky-Papkov et al., 2007)
	Hyaluronic acid and derivatives	Regeneration of skin, cartilage, Patterning of cell growth (Segura et al., 2005).
	Collagen-Hyaluronic acid gels	Control of vascular sprouting (Borselli et al., 2007).
	Chitosan	Chitosan microsphere-integrated scaffold, Cartilage engineering (Lee et al., 2004; Shi et al., 2006).
	Fibrin	Vessel engineering, Release of fibroblasts (Jeon et al., 2005; Ye et al., 2000).
	Gelatin	Trachea engineering, Bone engineering (Ito et al., 2003; Okamoto et al., 2004)
	Alginate	Vascular engineering (Perets et al., 2003).
Synthetic	PGA	Musculoskeletal tissue engineering (Day et al., 2004; Lutolf and Hubbell, 2005).
	PLA	
	PLGA	Cartilage regeneration, Fibrovascular engineering
	PCL	Skin engineering (Ng et al., 2001)
	Polyethylene glycol (PEG)	Bone formation (Lutolf et al., 2003).
Inorganic	Hydroxyapatite (HA)	Bone substitute (LeGeros, 2002; Paul and Sharma, 2003).

Polymer nanofibers have been fabricated using a number of different techniques. The methods of nanofiber fabrication are varied and utilize physical, chemical, thermal, and electrostatic fabrication techniques. The methods of polymer nanofiber fabrication most commonly associated with tissue engineering scaffolds in the literature are electrospinning, self-assembling peptide reactions, and phase separation (Ma et al., 2005; Vasita and Katti, 2006; Venugopal et al., 2008).

5.2.1. Electrospinning

It is generally agreed that electrospinning has the potential to produce scaffolds possessing the appropriate strength, nanoscalar structure, economic appeal, and

biocompatibility (Lannutti et al., 2007; Pham, Sharma, and Mikos, 2006). Some of its advantages and disadvantages are present in Table 7:

Table 7: Advantages and disadvantages of electrospinning process (adapted from Beachley and Wen, 2009).

	Advantages	Disadvantages
Electrospining	Easy to setup	Poor cell infiltration into the core of the scaffolds;
	Cost effective	2D pore or microstructure arrangement;
	High level of versatility allows control over fiber diameter, microstructure and arrangement	Toxic solvents often used.
	Vast materials selection	

Electrospinning is an ideal method for producing a network of fine fibers that mimic the *in vivo* ECM (Lannutti et al., 2007; Veleva et al., 2008). The fibrous structures produced by the electrospinning process have a high surface area to volume ratio providing enhanced cell response and potentially a higher cell density per unit volume compared to other structures (Veleva et al., 2008). Over the past decade, many natural and synthetic compositions have been electrospun in targeting specific biomedical applications (Veleva et al., 2008; Xu et al., 2004). Many different types of molecules can be easily incorporated during the electrospinning fabrication process to produce functionalized nanofibers (Beachley and Wen, 2009).

There are basically three components to fulfil the process: a high voltage supplier, a capillary tube with a pipette or needle of small diameter, and a metal collecting screen (Huang et al., 2003; Xie et al., 2010).

In the electrospinning process a high voltage is used to create an electrically charged jet of polymer solution or melt out of the pipette (Beachley and Wen, 2009; Huang et al., 2003). Before reaching the collecting screen, the solution jet evaporates or solidifies, and is collected as an interconnected web of small fibers (Deitzel et al., 2001; Fong and Reneker, 2001). One electrode is placed into the spinning solution/melt and the other attached to the collector. In most cases, the collector is simply grounded, as indicated in Figure 8 (Huang et al., 2003).

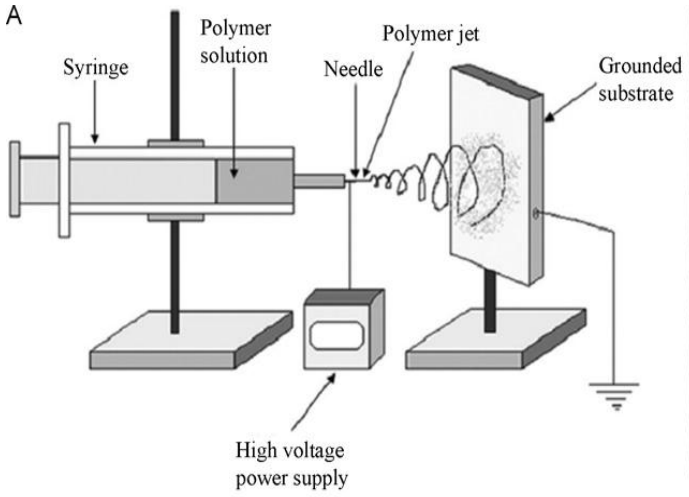

Figure 8: Manufacturing process of electrospinnig nanofibers (Beachley and Wen, 2009).

The electrospinning process seems to be the only method which can be further developed for mass production of one-by-one continuous nanofibers from various polymers (Huang et al., 2003).

Many parameters can influence the transformation of polymer solutions into nanofibers through electrospinning (Doshi and Reneker, 1995). These parameters include (Beachley and Wen, 2009; Doshi and Reneker, 1995):

a) the solution properties such as viscosity, elasticity, conductivity, and surface tension;
b) hydrostatic pressure in the capillary tube, electric potential at the capillary tip, and the gap (distance between the tip and the collecting screen); and
c) Solution temperature, humidity, and air velocity in the electrospinning chamber.

5.3. Tissue-inducing substances

Another important factor of tissue engineering is tissue-inducing substances, which include adhesion factors and growth factors. An adhesion domain discovered from fibronectin and other ECM proteins contains the amino-acid sequence of Arg-Gly-Asp (RGD), which may be engineered into the scaffold biomaterials to promote adhesion and control cell migration speed (Palecek et al., 1997).

Chapter II – Covering microchannels with electrospun nanofibers for cell discrimination

1. Introduction

Organ reconstruction and tissue regeneration are the main concern of tissue engineering. To accomplish this, many researchers work every day in many different areas, using cell culture, which has a key importance due to its high potential. The materials used in tissue engineering should offer total biocompatibility. They should have other properties like biodegradable and non-toxic, for example. The most common name for this cell supports are scaffolds or nanofibers in lower scale.

Many studies have been made with cell culture and nanofibers, almost all of them in a two dimensional structure, but recently the technology enabled three dimensional studies with help of microfluidic system. It is used the chips technology, in this case, photolithography, to build microchannels that allows simulation of *in vivo* properties.

Different types of devices can find a wide range of applications, including in pharmaceutical industry for drug studies, or for single cell study.

In this work, a microdevice was built with the initial purpose of placing nanofibers on specific chambers, and further on cells to observe their migration in nanofibers. The present chapter describes the methodology used, as also the results obtained and the corresponding discussion, including suggestions to improve the procedures and methods used. Finally, conclusions and recommendations were included in this chapter.

2. Methodology

This section is divided into 3 parts, one of which describes the steps and techniques used to draw and make the microchannels. Then, the techniques used to the microdevices adhere to a suitable surface were presented and finally, the process used to place cells inside of microchannels.

2.1. Design

The model was designed with AutoCad2010 software. In Figure 9, the wafer model and two enlarged devices are presented.

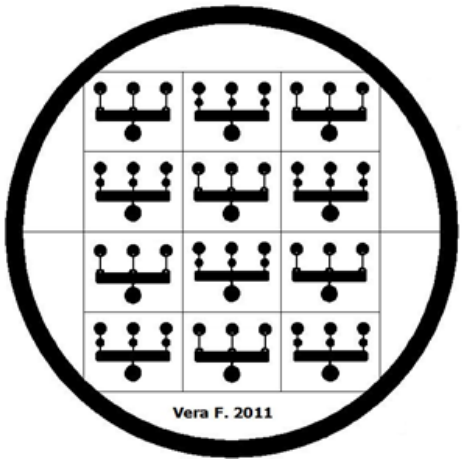

Figure 9: Drawing with two different microdevice models for print in waffer.

Both devices have 19 mm length and 14.5 mm width. Measurements of Device A and B are present on Table 8.

Table 8: Measures of microdevices A and B.

Device	Components		Measures [mm]
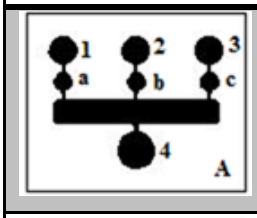	Chambers	1, 2, 3 cell inlet	3
		4 inlet/outlet	4
		a, b, c nanofibers	2
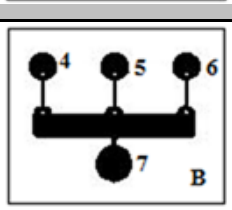	Channel	Length	0.2
		Width	3
	Chambers	4, 5, 6 cell inlet	3
		7 inlet/outlet	4

2.1.1. Photolithography, Protocol for 100 µm SU-8

Photolithography is the manufacturing process used to microfabrication of channels. To perform this procedure is necessary to use a clean room and as such all the procedures that this entails.

Before enter in clean room, it was prepared all the material to be used: reagents (H_2O_2 and H_2SO_4), wafers with 4 inch and photo masks. First it was turned on the equipment: UV exposer and laminar flow hood. Then wafers were cleaned with piranha solution (50% H_2O_2 + 50%H_2SO_4) for a total of 60 ml, during 5 minutes. The wafers were submerged in deionized water for 1.5 minutes. This step was done twice. Wafers were dried with an air gun and were place in spin coater for a few seconds, to ensure that they were dry. Next step was to place them on the hotplate at 200ºC for 20 minutes. Wafers were taken out and cooled for 5 minutes and then positioned in spin coater and deposited 4ml (1ml per inch) of the SU – 8 100 resin (photoresist) on centre of each wafer with the help of a pipette. The spin coater was turned on with speed of 500rpm over 15 seconds and then more 30 seconds at 3000rpm. Wafers were placed on a hotplate levelled for soft bake. They were baked for 30 minutes at 95ºC. Then, wait to cool on room temperature for 10 minutes. Mask was placed on UV exposer and aligned such as wafers for expose the photoresist to intense light. The machine was prepared to five cycles of one minute each. To conclude the procedure the wafers were placed in revealing solution twice for 8 minutes each. The wafers were submerged in isopropanol and was dried.

2.1.2. PDMS fabrication

To make moulds of microdevices using previous wafers made by photolithography, PDMS was chosen. To fabricate PDMS it was necessary to clean wafers with ethanol and then dry them with the help of a liquid nitrogen gun. It was used a mixer to do the PDMS. First it was placed in the container PDMS and curing agent in a 10:1 ratio. The mixer (Figure 10B) was turned on and the container was attached, mixing the PDMS and the curing agent during 3.30 minutes at 3000rpm. PDMS was placed inside the Petri dish on top of the wafer and to eliminate air bubbles it was used the vacuum box (Figure 10C). Let it rest for one day to solidify.

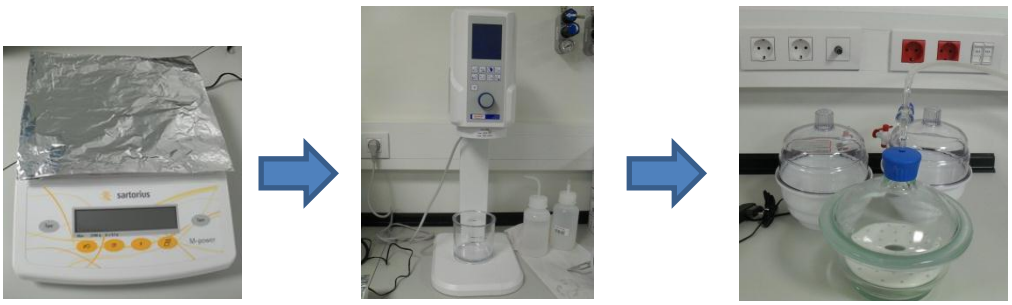

Figure 10: Manufacturing PDMS: (A) Balance; (B) Twister; (C) Desiccator.

2.2. Strategies to adhere PDMS on a substrate

It was necessary to adhere the PDMS on different substrates for discoverer the better material to do the experiences. The oxygen plasma method and the PDMS glue method are explained in next points.

2.2.1. Oxygen plasma method

Slide glass, PDMS device and plate wells were used. The oxygen plasma machine was turned on and the material was placed in the metal plate with the surfaces that it was necessary bond turned up. It was necessary adjust the pressure of machine to 0.75 bar, time 30 seconds and turned on. After completing the process material were taken out. At last, the PDMS was placed on the substrate (slide glass or plate wells) with careful and wait a little bit, depend of what materials we used.

2.2.2. PDMS glue method

PDMS was used as glue in this method. It was placed a thin layer of PDMS (not cured) on the substrate (plate wells or slide glass). Then it was placed the microdevice on the substrate with glue. Materials were placed in oven during 1h at 60ºC or 40ºC during 15 minutes.

2.3. Cell culture of Adipose-derived stem cells (ADSCs)

Green Fluorescent Protein (GFP) ADSCs were isolated from GFP-mice kindly provided by Dr. Prósper from Clínica Universidad de Navarra, Pamplona, Spain. (Mazo et al., 2008). Briefly, GFP adipose tissue cells were isolated from mice inguinal and interscapular adipose tissues. Inguinal fat pads were digested at 37 °C in DMEM-F12 (Invitrogen) containing 2% bovine serum albumin (BSA) and 2 mg/ml collagenase (Roche, Barcelona, Spain) for 30 min. After filtration (25 μm filters), mature adipocytes were separated from the stromal fraction by centrifugation (600×g for 10 min). The

pellet was re-suspended in culture medium and cells were then seeded (10,000 cells/cm^2) in DMEM-F12 with 10% Fetal Calf Serum (FCS) medium and maintained in 5% CO_2 and humidified atmosphere. Six hours after plating, all non-adherent cells were removed by washing. Sub-confluent ADSCs were obtained after 6 days. After trypsinization, the cells were counted and ready to use in further cell culture experiments.

2.4. Preparation of PCL electrospun scaffolds

PCL of which molecular weight were 80 kDa were purchased from Sigma–Aldrich (St Louis, MO, USA) and used without further treatment or purification. PCL solution with chloroform (Merck Chemical Co., Germany) was vigorously stirred with a magnetic stir bar for at least 24h at room temperature. Electrospinning was carried out at room temperature in a vertical spinning configuration, using a 1 mm inner diameter flat-end needle with a 10 cm working distance. The applied voltages were in the range from 10 to 13 kV, driven by a high-voltage power supply (Knürr-Heizinger PNC, Germany). The flow rates were adjusted with a programmable syringe pump (model 210, KD Scientific Inc., USA). The collector consisted of a 10 × 15 cm metal sheet covered in non-stick aluminum foil. To make two different densities of scaffolds, we collected fibers for low fiber density in 1 min (approximately 10 μm in thickness) and for high fiber density in 5 min (≤ 100 μm). All electrospinning processes were carried out under ambient conditions.

2.5. Scanning electron microscopy (SEM)

The size and morphology of the electrospun fibers were investigated by a scanning electron microscopy (Phenom G2 Pro Desktop Scanning Electron Microscope, Eindhoven, The Netherlands). The diameter of the fibers and their size distribution were analyzed by measuring over 200 fibers in randomly recorded SEM micrographs using an image analyzer (Image J, developed by the National Institute of Health, USA), for which the samples were directly electrospun on the aluminum foils. Scaffold thickness with different density and surface morphology of the electrospun fibers after incubation for 24h in phosphate-buffered saline (PBS) for the degradation tests were also investigated with SEM. All samples were attached to SEM mounts using carbon film, and then sputtered with gold to avoid overcharging.

3. Results and Discussion

The results are dividing in 3 parts. The first part has results of the photolithography process. Then, the second part has results obtained on the best option to adhere the PDMS devices on a substrate. The last part has the culture cells on microdevices, where it was described strategies used to place cells on devices.

3.1. Photolithography measurements

Microdevices in study were design with purpose to cover nanofibers scaffolds for cell discrimination (Figure 11). Because of this, it was necessary to make sure of its viability before placing nanofibers in microdevice.

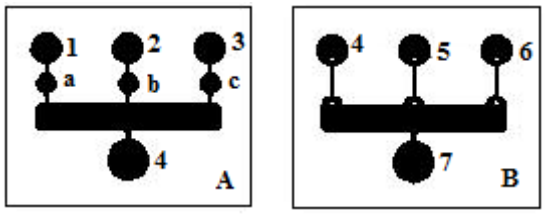

Figure 11: Microdevices (A) nanofibers in chambers a, b and c; and (B) nanofiber in channels.

First, it was necessary to ensure that the height was correct. So, after the process of photolithography, the measurements were made with Tencor. Table 9 shows the results obtained.

Table 9: Thickness of the cured resin

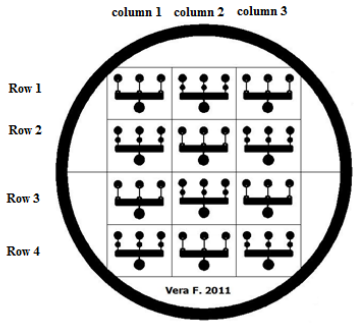

Location	Height
Row 1, column 2	~98µm
Row 1, column 3	~110µm
Row 3, column 3	~102µm
Row 4, column 1	~91µm
Row 4, column 3	~98µm
Average	99.8 µm

The height that was pretended was 100 µm. The photolithography process was successful, with an average of 99.8 µm. While not uniform, it did not presented significant discrepancies.

3.2. PCL electrospun fibers

The Figure 12 shows PCL fibers obtained by electrospinning described previously in this chapter on methodology.

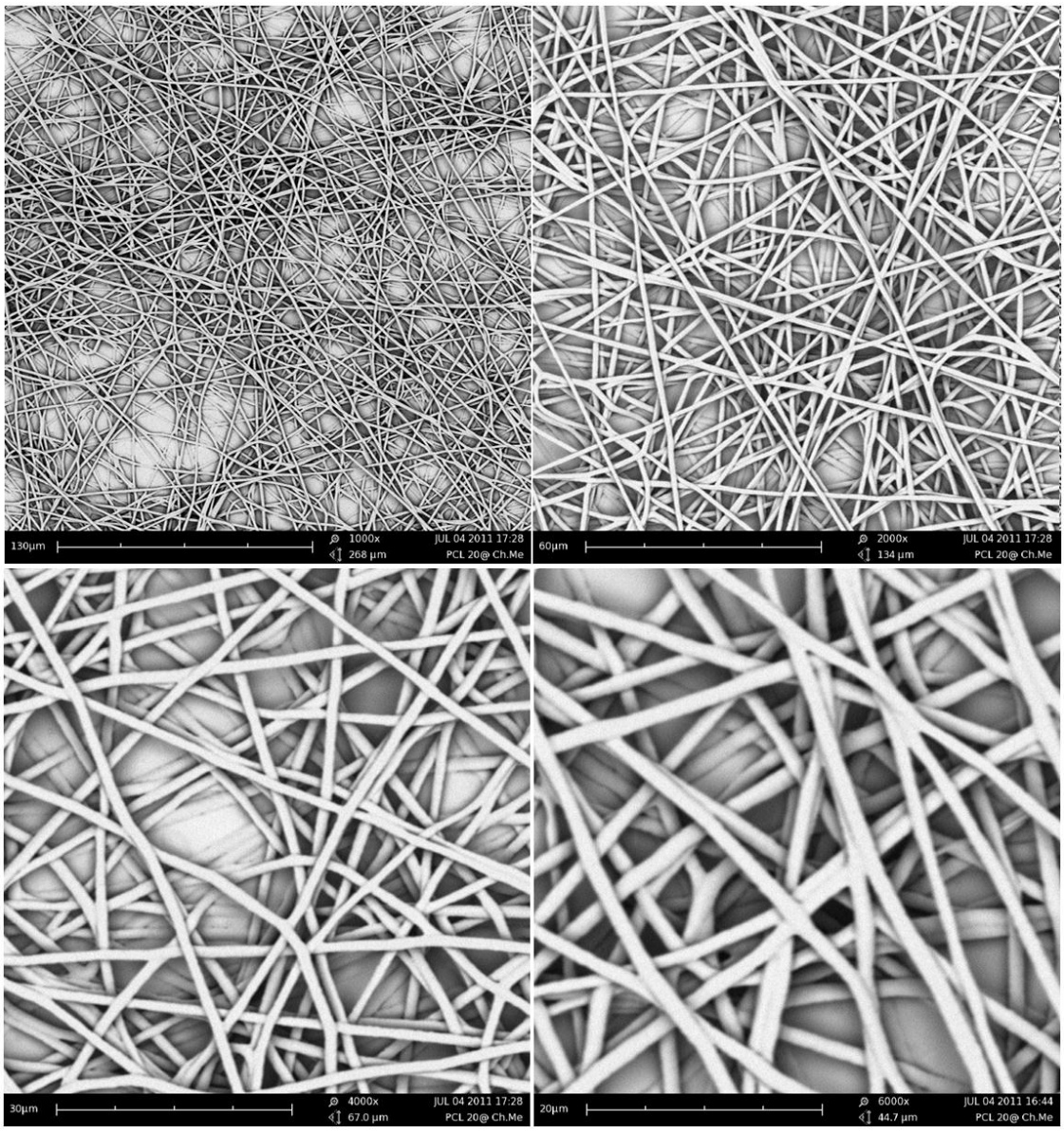

Figure 12: SEM pictures of PCL fiber (about 1µm) produce by electrospinning from the solution with Chloroform/Methanol 4/1 v/v (mixture solvent).

3.3. Strategies to adhere PDMS on a substrate

The strategies used show different results. In the next subchapters, the results and the best way chosen to adherence PDMS microdevice on a substrate will be presented.

3.3.1. Oxygen plasma method

Table 10 shows the procedure used to the adherence for culture dish and slide glass and the result obtained.

Table 10: Techniques used to adherence using oxygen plasma and procedure used.

Materials	Procedure	Results
Culture dish and device	Follow the protocol of machine and wait 18h.	Good adhesion between the materials
Slide glass and device	Follow the protocol of machine and wait 2h.	Good adhesion between the materials
Culture dish, device and nanofibers	Follow the protocol of machine and wait 18h.	Detach when placed medium in

The different materials used, culture dish and slide glass, had good results and proved to be a good option for the further experiences. However, slide glass was better because spent less time than the culture dish.

The possible advantage of culture dish is savings of medium (next subchapter shows this regarding evaporation of medium during culture).

3.3.2. PDMS glue method

Table 11 shows the procedure used to the adherence for culture dish and slide glass and the result obtained.

Table 11: Techniques used to adherence using PDMS glue and procedure used.

Materials	Procedure	Results
Culture dish, device and nanofibers	Step 1: place a thin layer of PDMS in plastic culture dish Step 2: place the nanofibers in PDMS layer Step 3: place the device in nanofibers Step 4: place everything in an oven 1h at 60ºC	The dish deform The channels of device were attaches It had many air bubbles Nanofibers degraded with the temperature
Slide glass, device and nanofibers	Step 1: place a thin layer of PDMS in a glass with a lamella Step 2: place the nanofibers and then the device Step 3 : place everything in oven during 15 minutes 40ºC	Good adhesion Few air bubbles Channels were not attaches

The PDMS glue method had worst results. When placed in the oven during one hour at 60ºC the dish culture deform and melt; device channels were attached to the dish culture and many air bubbles were observed.

The strategy that used the slide glass showed better results because the device channels were not attached and only a few air bubbles were visualized.

The best strategy when nanofibers are not used was oxygen plasma with slide glass substrate. But this strategy is not so good when cells were placed on the channels, because of the medium evaporation. On the case of culture dish, it was possible to place medium in less quantity.

To place nanofibers on device the strategy with glue PDMS method was better, despite some problems that occurred.

3.4. Cell culture in microdevice

3.4.1. Microdevice A

Microdevice A was used in first place. After the adhesion step it ensured that channels and chambers were clear and detached from slide glass. For this reason it was passed water into the microdevice it was found that all of chambers, channels and wholes were clear.

Second, it was chosen the flow rate. It was chosen a flow rate to place cells in chamber at 0.1 ml/h and filled the microdevice with medium 0.1 ml/min. Due to the small size of the device, flow rate had to be low to control the input of cells.

Third, it was necessary verify if cells migrate through channel, from chamber 2 to chamber b.

In this step several tests were made.

First test: Placed cells only in one chamber

Important data used in microdevice A:

- Flow rate for medium: 0.1 ml/min;
- Flow rate for cells: 0.1 ml/h;
- Filled time for cells: ~2 minutes.

It were followed these steps:

1. Was filled with cells in chamber 2;
2. Was filled with medium in chamber 4;
3. Were taken results photographically with epi-fluorescence microscope.

I was observed cells on the day that it was filled the device and the day after. The Figure 13 shows the result for day one.

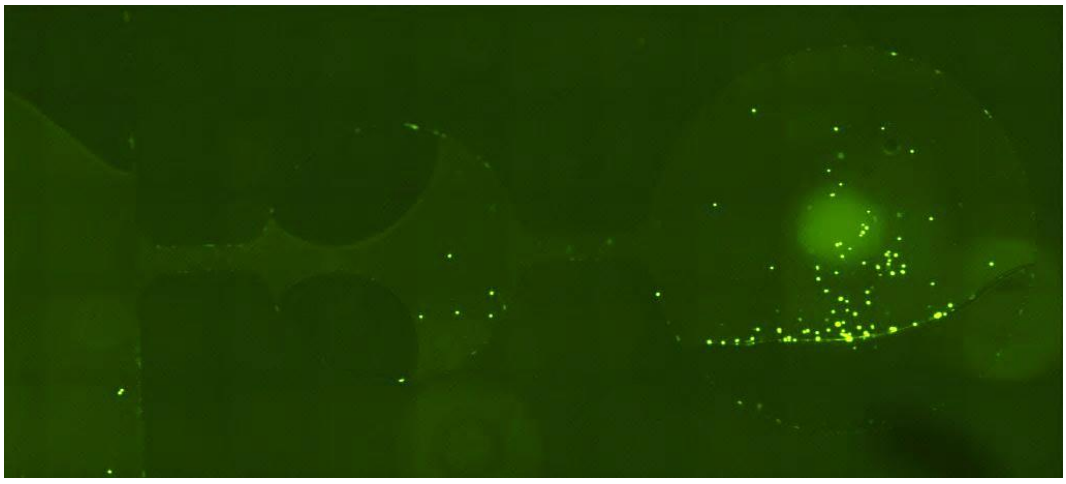

Figure 13: Cells filled - Chamber location: Chamber 2, b.

It was found that all chambers had many air bubbles, which is not good for the cells survive neither their migration. Using a pump to put booth cells as the medium proved to be very useful.

The microdevice A was placed in the incubator for 24 hours to preserve good health of cells and the result of that was the evaporation of medium. One reason for this is the holes, which were made to place the medium and cells, and the temperature of the incubator. One possible solution would be covering channels with a slide glass.

Second test: Placed cells only in one chamber

Important data used in the microdevice A:

- Flow rate for medium: 0.1 ml/min;
- Flow rate for cells: 0.1 ml/h;
- Filled time for cells: ~5 min.

It was followed these steps in this experiment:

1. Was filled with medium in chamber 4;
2. After all the device was filled with medium, cells were placed in the chamber 1 during 5 minutes, because chamber 2 was blocked;
3. Were taken results photographically with epi-fluorescence microscope.

I was observed cells on the day that it was filled the device and in the day after. The Figure 14 shows the result to day one.

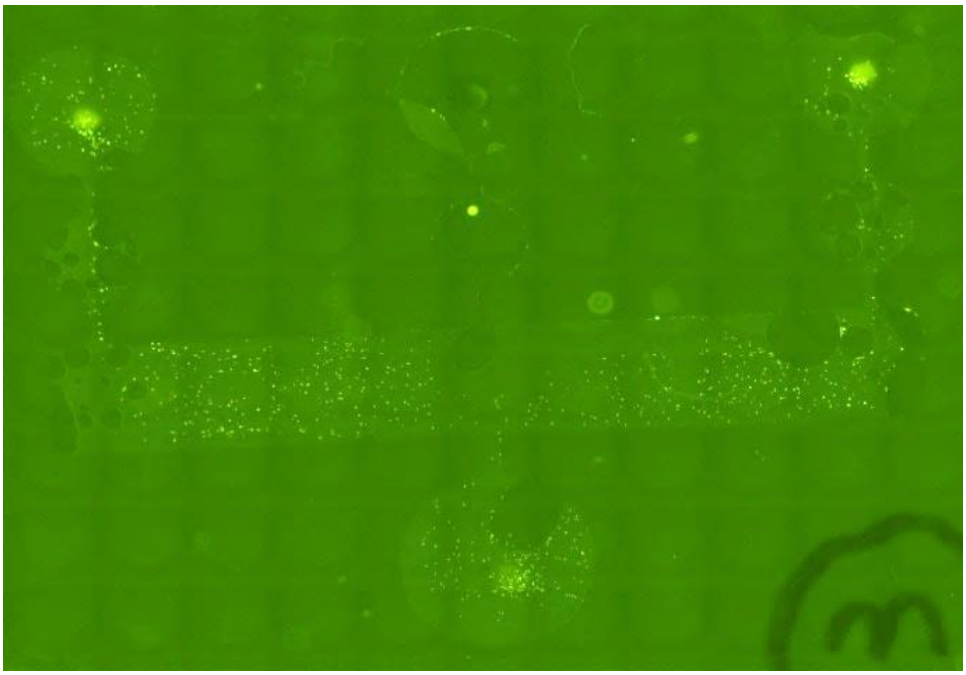

Figure 14: Cells filled - Chamber location: Chamber 1, b.

The results were taken 4h after filling the microdevice with cells. It was observed that cells are in almost all of the device, with the exception of the middle chambers. So 5 minutes to fill the chamber with cells was too much time.

In the next day, 24h after, almost all cells died, Figure 15.

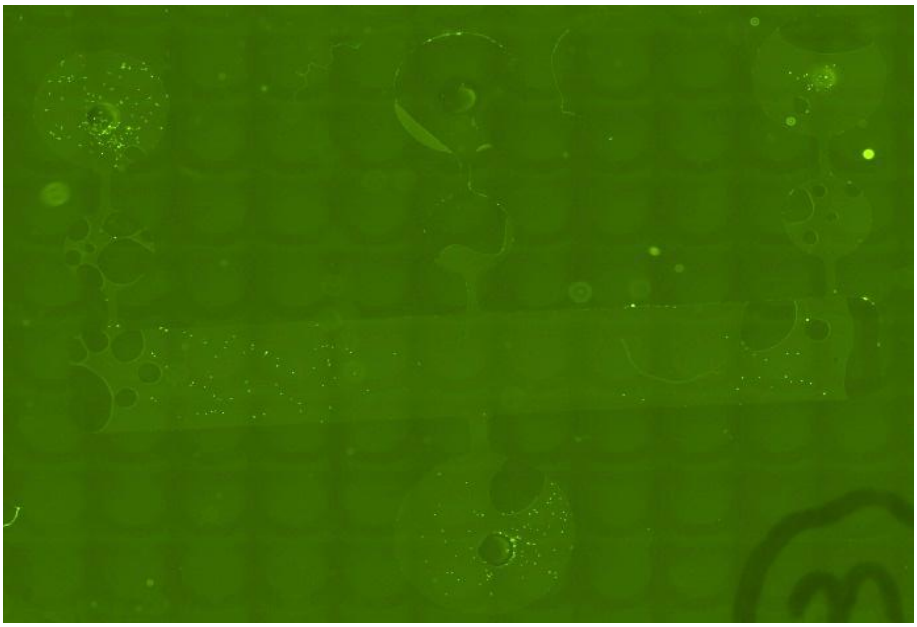

Figure 15: 24h after filled chamber with cells.

In Figure 15 it was possible see cells in chambers 1, 3, 4 and the medium did not evaporate like last time. Cover-glass the device was able to prevent the medium evaporation. It was found that some cells were attached in different areas, as shown in Figure 16.

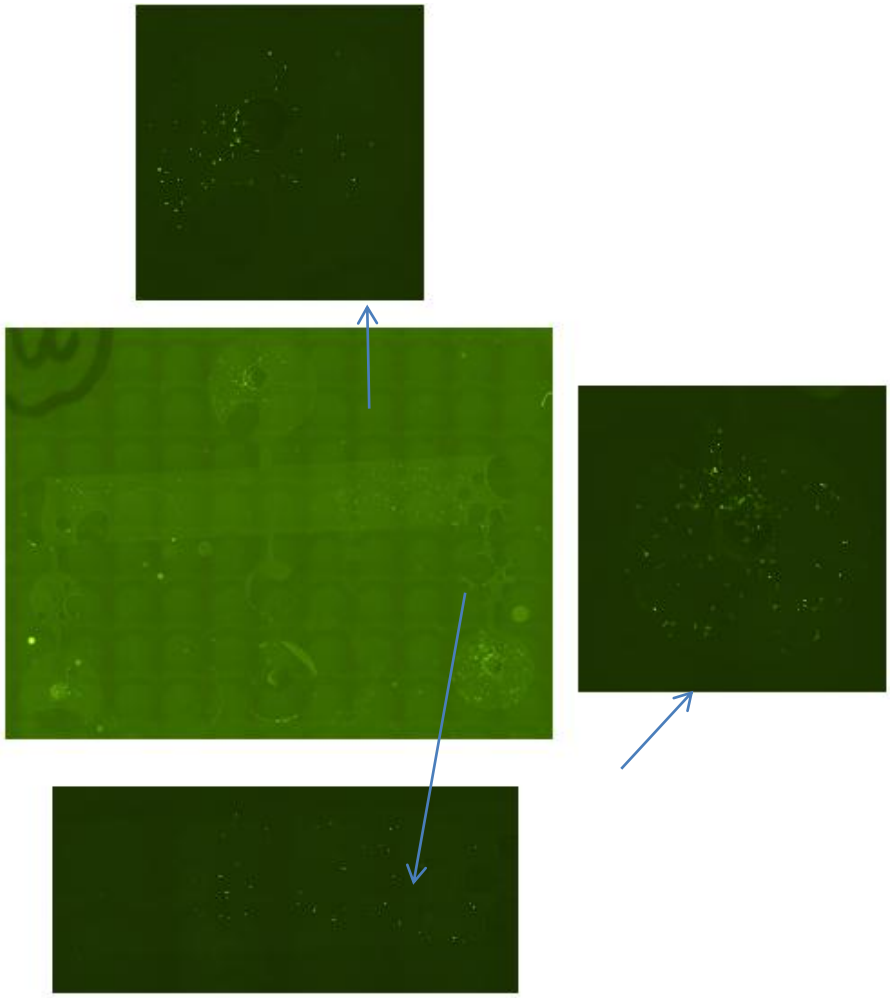

Figure 16: Images from cells found in microdevice A, in second test.

Third test: Placed cell only in one chamber

Important data used in the device 3:

- Flow rate for medium: 0.1 ml/min;
- Flow rate for cells: 0.1 ml/h;
- Filled time for cells: 1 min.

It was followed these steps in this experiment:

1. Was filled with medium in chamber 4;
2. After all the device was filled with medium, placed cells in the chamber 2 during 1 minutes;
3. Were taken results photographically with epi-fluorescence microscope.

It was observed cells on the day we filled the device and in the day after. The Figure 17 shows the result.

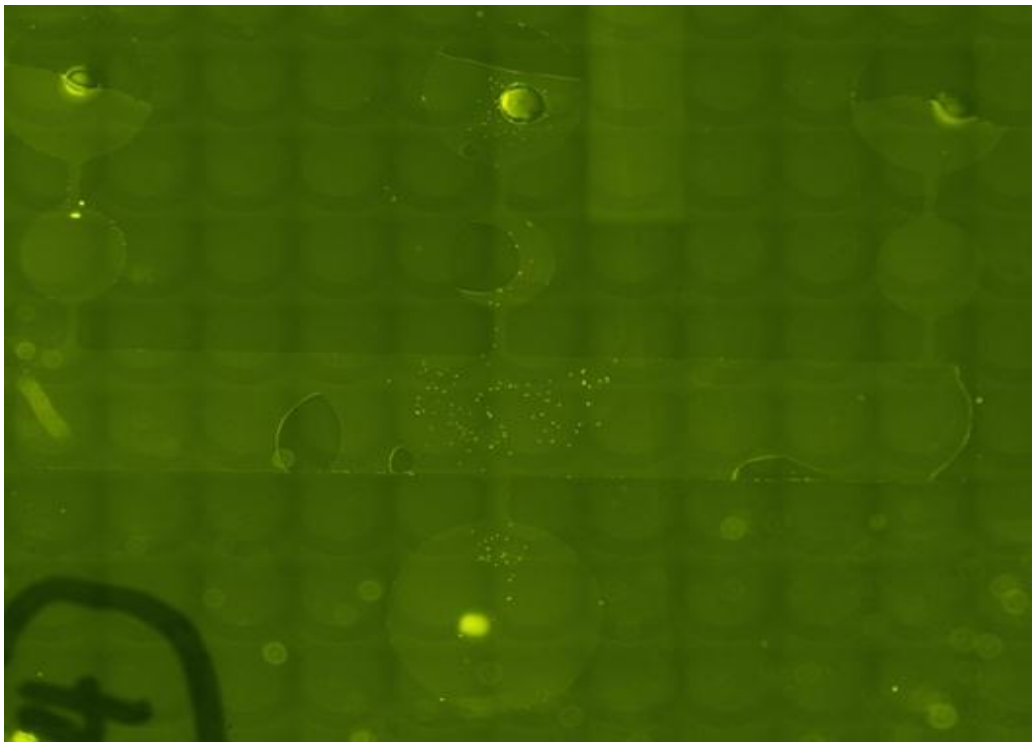

Figure 17: Cells in microdevice A, 4h after filled.

In this test we only had cells in centre of device, chamber 2, b, 4.

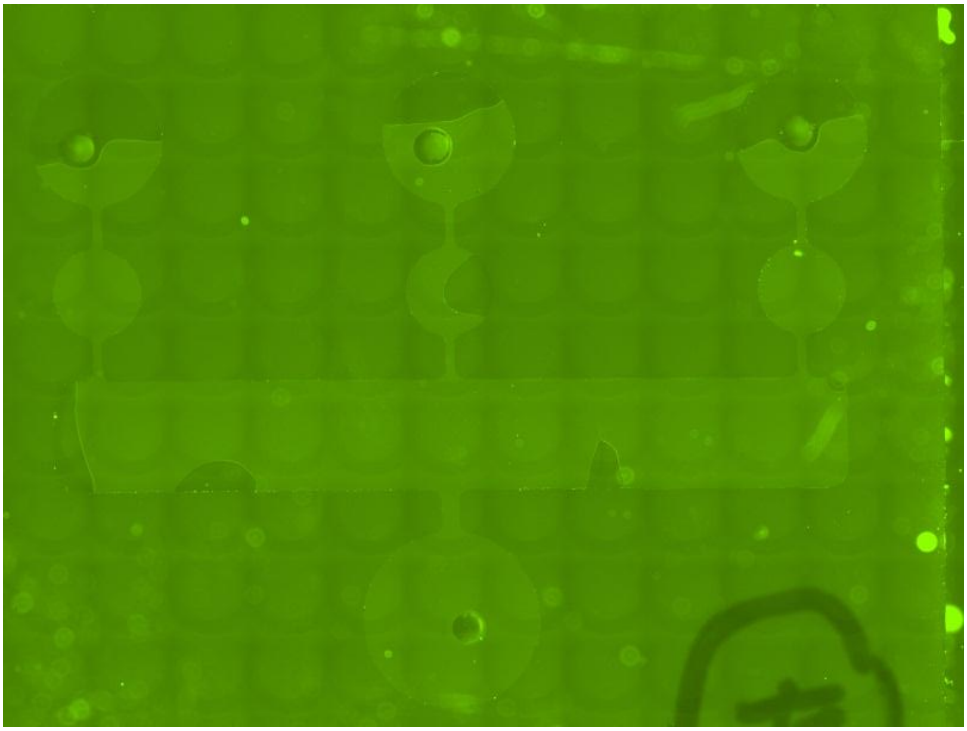

Figure 18: cells on microdevice A, 24h after filled.

This procedure was more successful with regard to placement of cells, however, it was only necessary to place cells in the chamber 2, and that was not obtained.

4. Conclusions and Recommendations

The oxygen plasma was the technique to adhere PDMS to a substrate that gave good results. But, when nanofibers were placed on the device this choice was not so good, because the nanofibers are very thin and flexible and it was difficult to work with them in a short period of time. The oxygen plasma only have half an hour to bounding the materials and it is a short period to place nanofibers in proper local and bonding the material.

Seeding cells on devices was another challenge, and was verifying that the pump with a flow rate and time controlled was a viable choice.

Beside all this issues, the other geometry was not tested. It was suggested another device design. The new geometry design has two layers that would be a good solution to insert the nanofibers and cells without initial problems obtained on first geometry, respectively when nanofibers were placed. Controlling the cell entrance is very important, and this geometry could help us, because it was possible to place cells with different inlet. Furthermore, in this new geometry, the height of channels and chambers was different.

Chapter III – Effect of tumour cells on deformability of erythrocytes

1. Introduction

Nowadays, cancer is the most popular and mortal disease and therefore, the investigation for understanding its proliferation and how it is possible to control and treat the disease are very important.

"Membrane of Red Blood Cell will be modified in contact with tumour cells?", this is the question that emerges. We know that erythrocytes of diabetic people have a rigid membrane compared with normal people. So, is it possible that the same thing occurs when people have tumours?

In this chapter different biomedical devices were tested in order to achieve the proposed objectives and overlap some difficulties. The microdevices described in the previous chapter were firstly applied. The first barrier was the adhesion of the PDMS device with any substrate. The second obstacle was the good adherence of cells on microdevice. Therefore, it was decided to use tumour cells to evaluate their influence in the deformability of erythrocytes. To be able to see deformation, a specific device presented on Figure 19 was used.

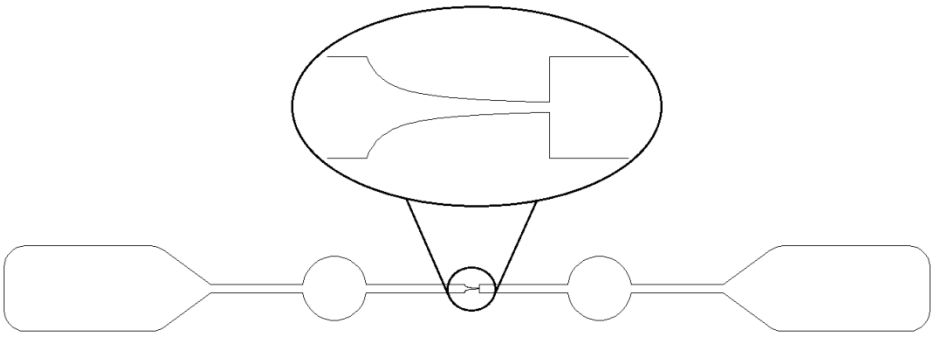

Figure 19: Deformation microchannel with 20 µm of width.

The present chapter describes the methodology used, and also the results obtained and the corresponding discussion, including suggestions to improve the procedures and methods used. Finally, conclusions and recommendations were included in this chapter.

2. Methodology

In this section the procedures used to evaluate deformability of RBCs in the presence of tumour cells are described.

2.1. PDMS glue method

PDMS was prepared with a proportion of 20:1. A glass slide was placed on spin coater vacuum. A portion of PDMS previously prepared was placed on slide glass. The spin coater was turned on with following program: 3000rpm, during one minute and 4000rpm, during one more minute. After finish program the slide glass was taken out and placed in the oven during 10 minutes at 80ºC. After the specific time the PDMS device was placed on slide glass and placed again in the oven during 24h.

2.2. Surface modification and adhesion with piranha and KOH solution

To prepare 50 ml of 1M KOH solution, 3.2060 g of KOH were dissolved in 50 ml of water.

To prepare 50 ml of piranha solution (2:3), 30 ml of H_2SO_4 was placed in a recipient and then slowly and very careful H_2O_2 was added to the same recipient. Microdevices were placed in piranha solution during 15 minutes and mixed from time to time. After 15 minutes, microdevices were removed and rinsed with deionized water. Then, microdevices were placed in KOH solution for the same period and, after this, rinsed with DI water. Microdevices were placed in oven at 80ºC during 4h.

2.3. Preparation of erythrocytes

2.3.1. Bovine blood

The bovine blood was collected, divided in two falcon tubes and centrifuged 20 minutes at 1200rpm. After this, the plasma (supernatant) was removed and mixed with HBSS (twice of volume). It was centrifuged again for 5 minutes at 1200 rpm and plasma was removed again. The procedure was repeated 3 more times. In the end, the plasma was removed, mixed with HBSS and centrifuged for 10 minutes at 1200rpm.

2.3.2. Human blood

Human blood was collected, divided in two falcon tubes and centrifuged 10 minutes at 1000 rpm. After this, the plasma was removed, mixed withed HBSS and centrifuged again 10 minutes at 1000rpm. The plasma was removed again and resuspended in HBSS at a known concentration (2%).

2.4. Culture medium preparation

To prepare 100 ml of medium, RPMI 1640 (87 ml) was supplemented with fetal bovine serum (10% FBS, 10 ml), 100 U/ml streptomycin/penicillin antibiotic (1 ml), 2 mM glutamine (1 ml), and essential amino acids (1 ml) and further heated at 37ºC.

2.5. Cell culture

Two human tumour cell lines were used: NCI-H460 (non-small cell lung cancer) and HCT-15 (colon carcinoma). Cells were routinely maintained as adherent cell cultures in culture medium previously described, at 37ºC, in a humidified air incubator containing 5% CO_2. Each cell line was plated at an appropriate density (2×10^5 cells/well for NCI-H460 and HCT-15) in 6-well plates and mixed with 1 ml of erythrocytes (2% Htc). One sample erythrocytes was taken after 24h of incubation and another one after 48h.

2.5.1. Assessment of cells growth inhibition using Sulforhodamine B colorimetric assay

After the culture period (24 or 48h), the adherent cells were fixed by adding cold 10% trichloroacetic acid (TCA, 100 µl) and incubated for 60 minutes at 4 ºC. Plates were then washed with deionized water and dried; sulforhodamine B solution (0.1% in 1% acetic acid, 100 µl) was then added to each plate well and incubated for 30 min at room temperature. Unbound SRB was removed by washing with 1% acetic acid. Plates were air dried, the bound SRB was solubilised with 10 mM Tris (200 µl) and the absorbance was measured at 540 nm in a microplate reader.

2.6. Deformability and recuperation tests for large channel

To evaluate the deformability of erythrocytes that were in contact with tumour cell lines, a channel was used (Figure 20).

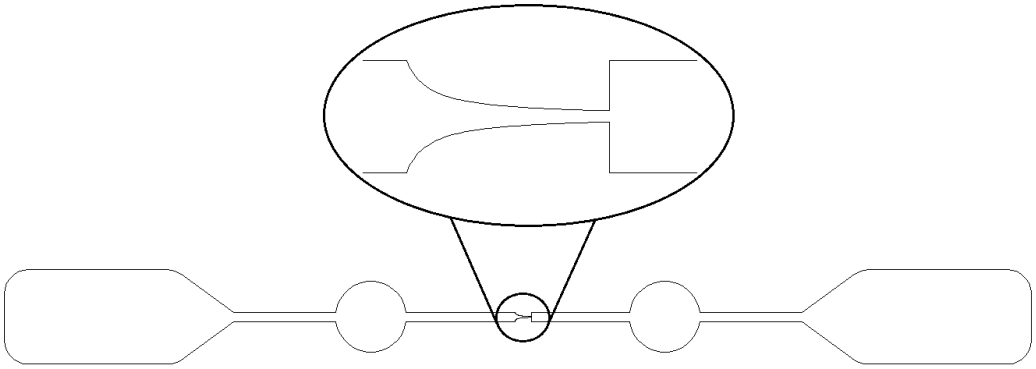

Figure 20: Geometry used to test deformability of erythrocytes.

For this study, 6 sections were defined on the channel (Figure 21).

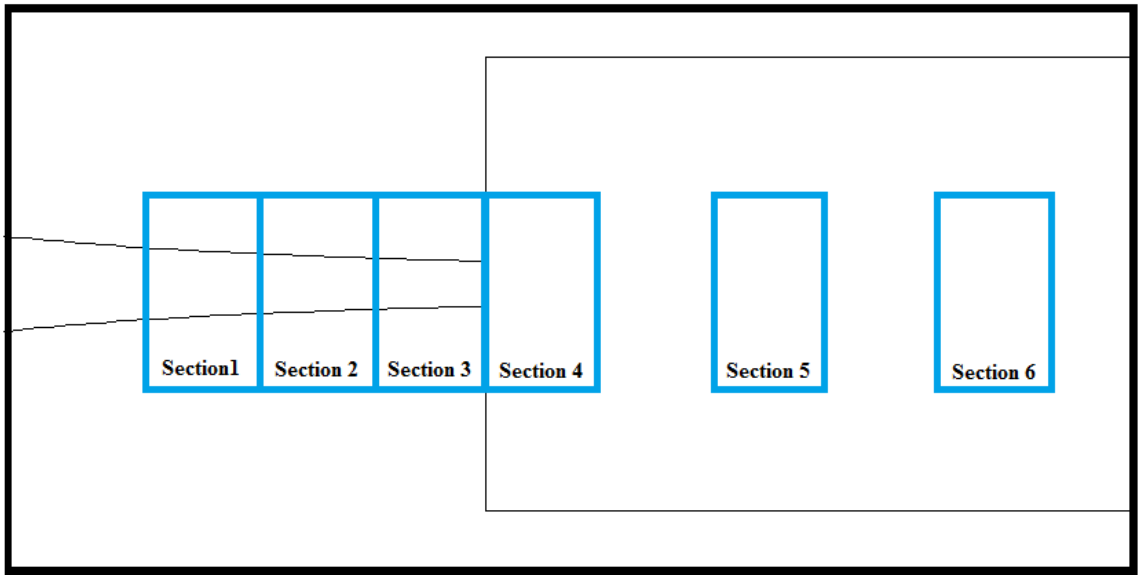

Figure 21: Sections defined on the channel used in the present study.

The most important sections were the first ones, where the deformation occurs. Section 5 and 6 were only to see recuperation of erythrocytes.

3. Results and Discussion

The devices made on CEIT and described in chapter II were firstly used to perform cell culture. Nevertheless, some problems occurred regarding the adhesion of PDMS to glass plate (the technique used to the adherence was the PDMS glue method, described on the previous section). Problems to place cells on device were observed– the PDMS is hydrophobic, and because of that cells do not attach. It was necessary to find another way to make adhesion between PDMS and glass, in order to make it hydrophilic. Maji et al. (2012), performed a study of hydrophobicity and stability of chemically modified PDMS surface using piranha solution and KOH solution. They tested three different ways to make PDMS hydrophilic and measure the contact angle, using FTIR to confirm results.

To change the surface of PDMS, their procedure was followed (described on the previous section). Besides changing the surface of the PDMS, it may also be used to create adhesion. Therefore, it was tried adhesion between PDMS and glass, and PDMS and petri dish culture.

The cells were prepared and placed on the changed devices. After one day, the cells were dead. So, the surface modification was temporary and takes only a few hours. Even if the cells were able to adhere, after a few hours they were repelled by the device and died.

In this way, different devices were used to study deformability of erythrocytes, after contact with human tumour cells.

3.1. Deformability of erythrocytes

The next experiments were performed using bovine and human erythrocytes.

3.1.1. Experiment 1 - Bovine erythrocytes

The device had 14 μm of height.

To obtain images and videos, an Olympus camera attached to an inverted optical microscope. It was very difficult to observe bovine erythrocytes. Figure 22 shows an example of quality of images that was possible to obtain.

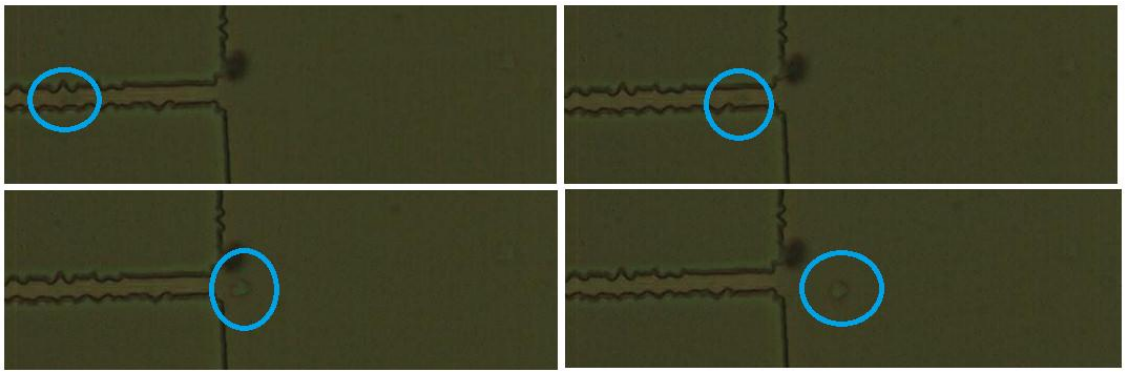

Figure 22: Erythrocyte images captured at 2000fps, 40x +1.6 x zoom with a flow rate of 100nl/min.

The blue circle indicates the location of erythrocytes, being evident their bad definition. With 2000fps, the light was lost being only possible to see the erythrocyte when they had already passed the channel. To see deformation it is required to see erythrocytes in the channel.

The control of the flow rate on the channel was another important difficulty. The pump was defined for the minimum flow rate, 100 nl/min, but probably it was too much because the erythrocytes crossed very fast. Nevertheless, it is still visible that some cells do not deform.

Because of all these issues the human erythrocytes were chosen as a sample fluid.

3.1.2. Experiment 2 – Human erythrocytes

For this experiment, the video camera was changed. All videos were taken with canon film camera, fixed on an inverted optical microscope. The important options made for the videos were the frames per second, 7500, the recording window, 1024x256, the objective, 20x with precision 0.75 and the velocity of the flow, 500 nl/min.

The videos were treated on ImageJ software following the steps presented below.

First the videos were opened in ImageJ software and converted to sequences of JPEG images (stack). Then, the image stack was opened the sequentially and incremented by 4 at the same time as shown in Figure 23.

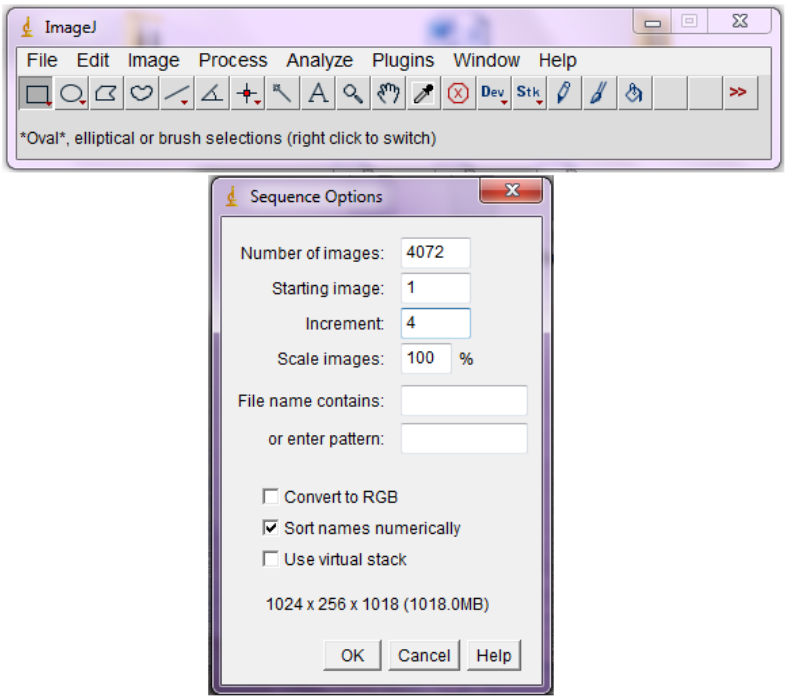

Figure 23: ImageJ software image sequence operation.

The next step was calibrating the images. The minimum distance of the channel at the exit of contraction part, known as 20µm, was used as a reference to calibrate and 2.100 pixels/µm was set as a scale (see Figure 24).

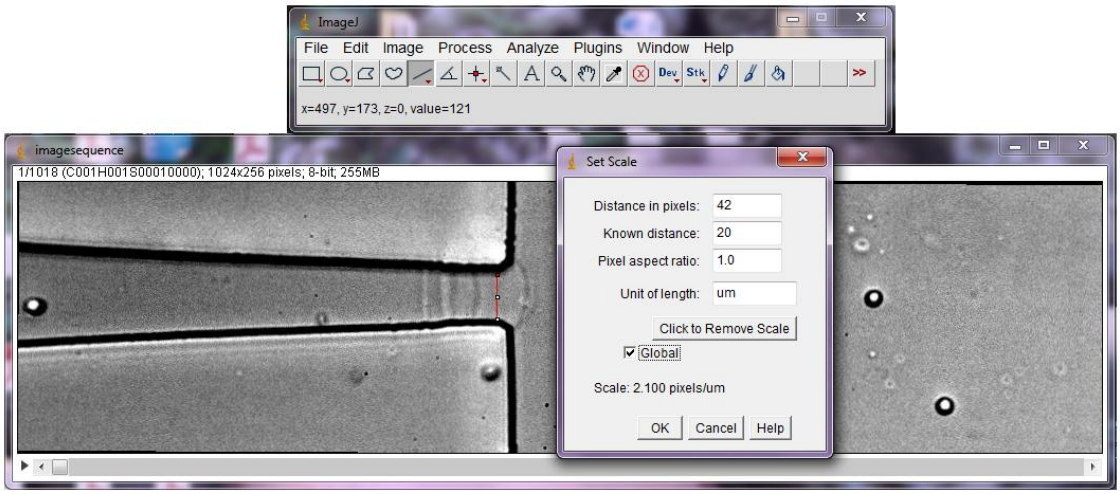

Figure 24: Image calibration in ImageJ.

After calibration, it was necessary to rotate the images slightly, because they were not horizontally aligned. The angle of rotation could be different according to the images. Then, a background image was created applying median operation to the stack, by using ImageJ function Z-project. The background image contains only static objects such as microchannels walls and noises as shown in Figure 25.

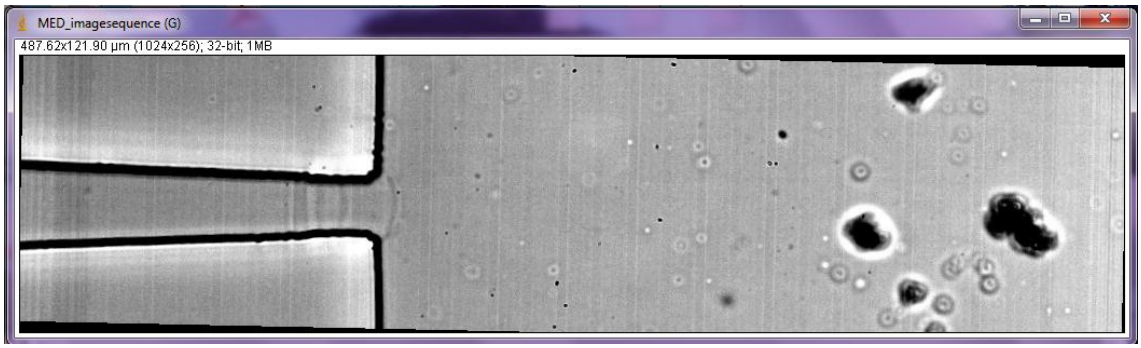

Figure 25: Background image.

This image was used to subtract from the original image with the ImageJ function Image Calculator (see Figure 26).

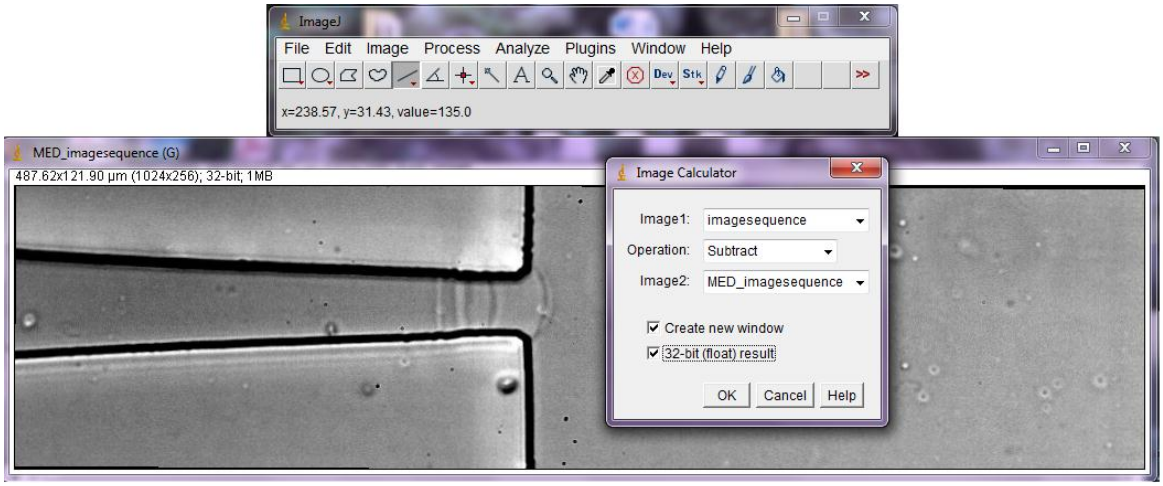

Figure 26: Step of Image Calculator.

The image obtained from the procedure above is presented in Figure 27. In this image only flowing RBCs are visible.

Figure 27: Subtracted image.

The brightness and contrast were adjusted to ensure the good definition of erythrocytes and then Otsu threshold method was applied (see Figure 28).

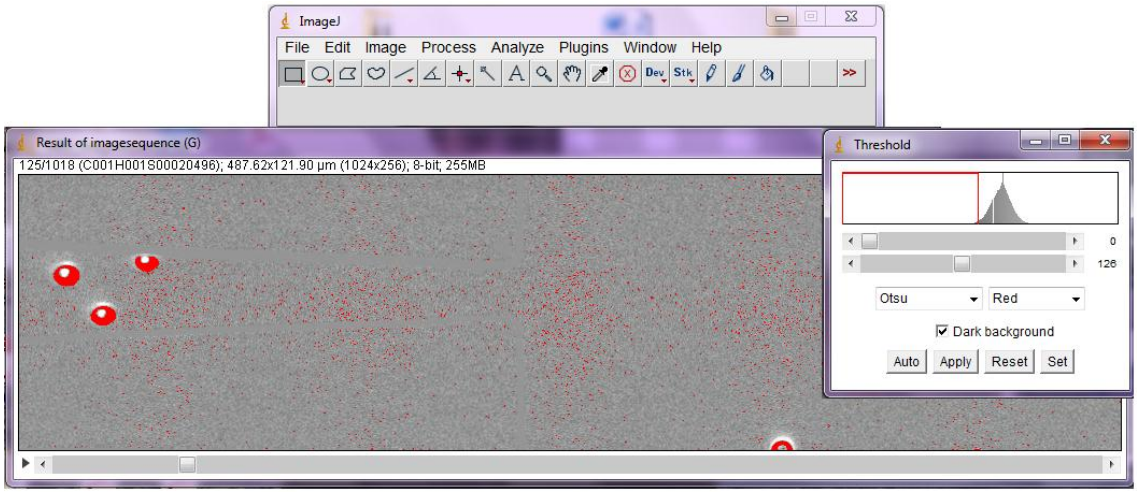

Figure 28: Threshold options step.

After this operation, the images were transformed in black and white (binary images). Finally, RBCs were measured by ImageJ function Analyze Particles (see Figure 29).

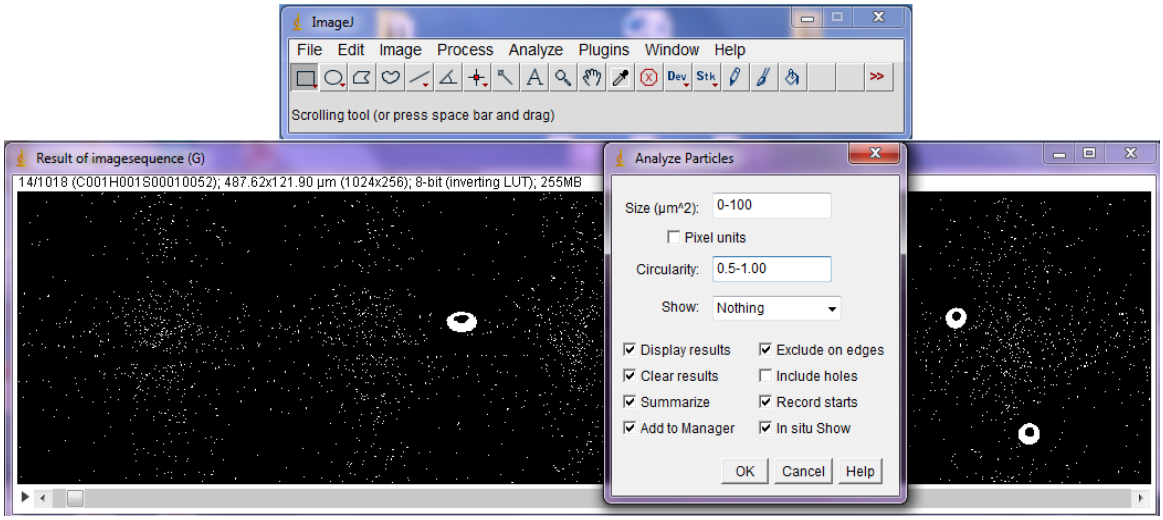

Figure 29: Options to analyze particles.

The program runs and flowing RBCs were measured frame by frame, and the results were recorded as a table as shown in Figure 30.

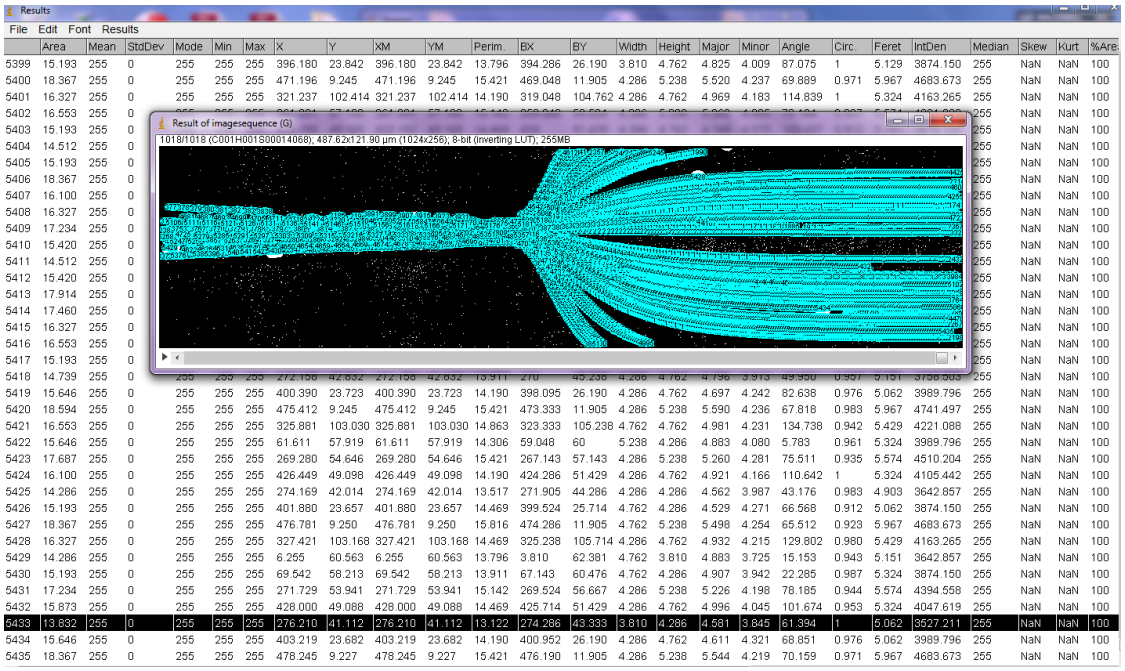

Figure 30: Results table and image results.

The table of results contains many measurements elements (columns) and for the current studies several elements were used, that are presented in Figure 31 in the orange rectangles.

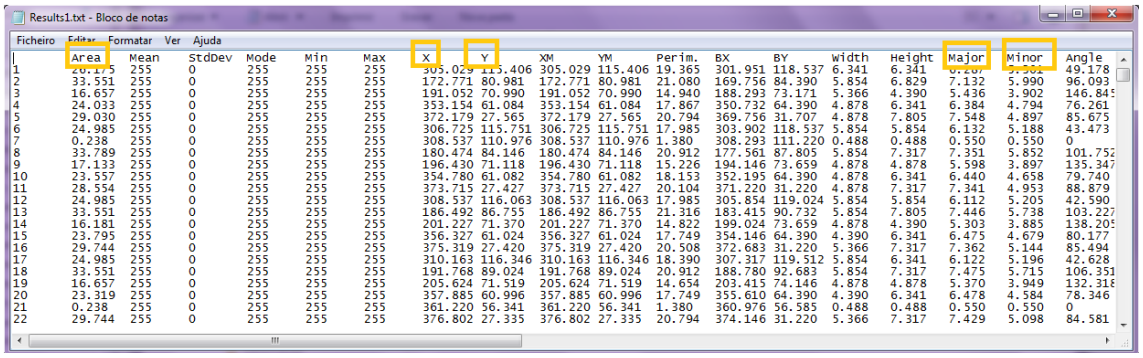

	Area	Mean	StdDev	Mode	Min	Max	X	Y	XM	YM	Perim.	BX	BY	Width	Height	Major	Minor	Angle
1	20.175	255	0	255	255	255	305.029	113.406	305.029	115.406	19.365	301.951	118.537	6.341	6.341	6.707	3.902	49.178
2	33.551	255	0	255	255	255	172.771	80.981	172.771	80.981	21.080	169.756	84.390	5.854	6.829	7.132	5.990	96.093
3	16.657	255	0	255	255	255	191.052	70.990	191.052	70.990	14.940	188.293	73.171	5.366	4.390	5.436	3.902	146.845
4	24.033	255	0	255	255	255	353.154	61.084	353.154	61.084	17.867	350.732	64.390	4.878	6.341	6.384	4.794	76.261
5	29.030	255	0	255	255	255	372.179	27.565	372.179	27.565	20.794	369.756	31.707	4.878	7.805	7.548	4.897	85.675
6	24.985	255	0	255	255	255	306.725	115.751	306.725	115.751	17.985	303.902	118.537	5.854	5.854	6.132	5.188	43.473
7	0.238	255	0	255	255	255	308.537	110.976	308.537	110.976	1.380	308.293	111.220	0.488	0.488	0.550	0.550	0
8	33.789	255	0	255	255	255	180.474	84.146	180.474	84.146	20.912	177.561	87.805	5.854	7.317	7.351	5.852	101.752
9	17.133	255	0	255	255	255	196.430	71.118	196.430	71.118	15.226	194.146	73.659	4.878	4.878	5.598	3.897	135.347
10	23.557	255	0	255	255	255	354.780	61.082	354.780	61.082	18.153	352.195	64.390	4.878	6.341	6.440	4.658	79.740
11	28.554	255	0	255	255	255	373.715	27.427	373.715	27.427	20.104	371.220	31.220	4.878	7.317	7.341	4.953	88.879
12	24.985	255	0	255	255	255	308.537	116.063	308.537	116.063	17.985	305.854	119.024	5.854	5.854	6.112	5.205	42.590
13	33.551	255	0	255	255	255	186.492	86.755	186.492	86.755	21.316	183.415	90.732	5.854	7.805	7.446	5.738	103.227
14	16.181	255	0	255	255	255	201.227	71.370	201.227	71.370	14.822	199.024	73.659	4.878	4.390	5.303	3.885	138.205
15	23.795	255	0	255	255	255	356.327	61.024	356.327	61.024	17.749	354.146	64.390	4.390	6.341	6.475	4.679	80.177
16	29.744	255	0	255	255	255	375.319	27.420	375.319	27.420	20.508	372.683	31.220	5.366	7.317	7.362	5.144	85.494
17	24.985	255	0	255	255	255	310.163	116.346	310.163	116.346	18.390	307.317	119.512	5.854	6.341	6.122	5.196	42.628
18	33.551	255	0	255	255	255	191.768	89.024	191.768	89.024	20.912	188.780	92.683	5.854	7.317	7.475	5.715	106.351
19	16.657	255	0	255	255	255	205.624	71.519	205.624	71.519	14.654	203.415	74.146	4.878	4.878	5.370	3.949	132.318
20	23.319	255	0	255	255	255	357.885	60.996	357.885	60.996	17.749	355.610	64.390	4.390	6.341	6.478	4.584	78.346
21	0.238	255	0	255	255	255	361.220	56.341	361.220	56.341	1.380	360.976	56.585	0.488	0.488	0.550	0.550	0
22	29.744	255	0	255	255	255	376.802	27.335	376.802	27.335	20.794	374.146	31.220	5.366	7.317	7.429	5.098	84.581

Figure 31: Results table and the elements used for analyses.

The first column is the sequential ID number assigned to the erythrocytes which were measured in each frame. The second one is the area of particle, and then X and Y presents the center position of particle, Major and Minor are the major and minor axis lengths of an ellipse that best fits the particle.

In order to use only necessary data, the results were treated by the following stages.

(1) The minimum area was set to be 10 μm^2 to eliminate errors from the results

(2) X corresponds to the length of channel and it was divided into 6 sections for analyses (see Figure 21), so X is limited to these sections.

(3) Y is the width of the channel and it is limited, too. Sections 1-4 have 14 µm in middle of channel. The other sections do not have limit.

(4) DI (deformation index) is calculated by following the equation in Figure 32. X and Y correspond to Major and Minor respectively.

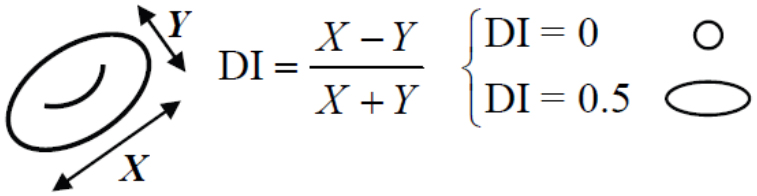

Figure 32: Definition of deformation index (DI).

For this experiment, a work plan was made and its resume is in Table 12.

Table 12: Resume table of work plan.

	0h	**24h**	**48h**
Human Erythrocytes	Case 1	Case 2	Case 3
Human Erythrocytes + HCT15*	-	Case 4	Case 5
Human erythrocytes + NCI-H460*	-	Case 6	Case 7

* tumour cell lines

For each case, several videos were recorded to observe erythrocytes deformation for 2% haematocrit (Hct):

Case 1: Erythrocytes with HBSS, ambient temperature control

Case 2: Erythrocytes with medium, 24h, 37ºC, 5% CO_2

Case 3: Erythrocytes with medium, 48h, 37ºC, 5% CO_2

Case 4: Erythrocytes in contact with HCT - 15, 37ºC, 5% CO_2

Case 5: Erythrocytes in contact with HCT - 15, 48h, 37ºC, 5% CO_2

Case 6: Erythrocytes in contact with NCI-H460, 24h, 37ºC, 5% CO_2

Case 7: Erythrocytes in contact with NCI-H460, 48h, 37ºC, 5% CO_2

Videos of each case were compared to know which one better represent the expected behaviour of erythrocytes in the channel.

The comparison of videos for case 1 was represented in Figure 33.

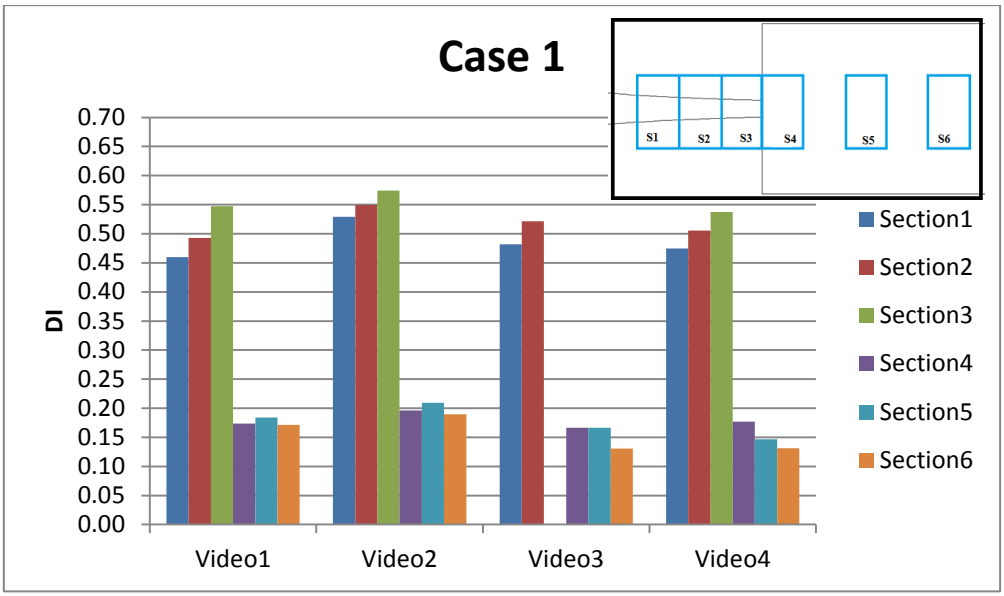

Figure 33: Comparison of DI for all videos in Case 1 in each section.

It was expected more deformation in section 3 than in the other sections as it is right before the exit part of the contraction part in the channel. The videos that show the ideal behaviour of erythrocytes in the channels are videos 1, 2 and 4. Video 3 have a missing value that corresponds to section 3. This was due to the number of RBCs being greatly reduced in some samples and also the method used to make the measurements. In our case it was the automatic method described early in this chapter.

In the first 3 sections in all of videos it is possible to see the expected behaviour of RBCs, an increase of DI. In section 4, 5 and 6 it was expected a decrease of DI and this is observed too, in all of videos.

Figure 34 shows the comparison between all videos of case 2.

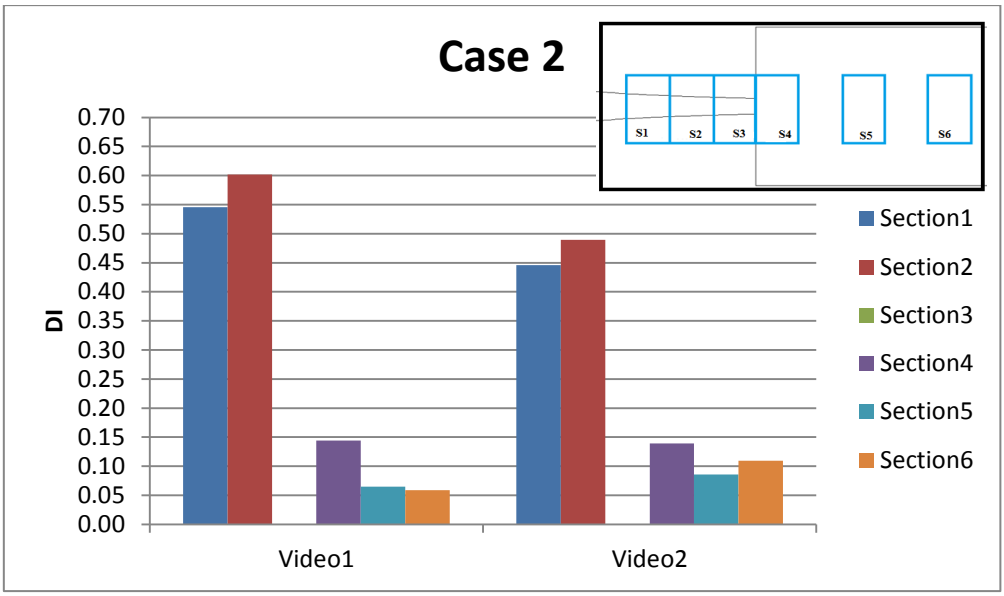

Figure 34: Comparison of DI for all videos in Case 2 in each section.

Video 1 and 2 does not have the section 3. Among all the videos it was impossible to choose one because section 3 (the most important section to see maximum deformation) is missing in all the cases. However, there can be seen a tendency that DI increases from section 1 to 2, and decreases dramatically at section 4.

The missing values are not present because of the explained reasons in the case 1 (very few RBCs and the used method to measure DI).

Figure 35 gives the comparison between videos of case 3.

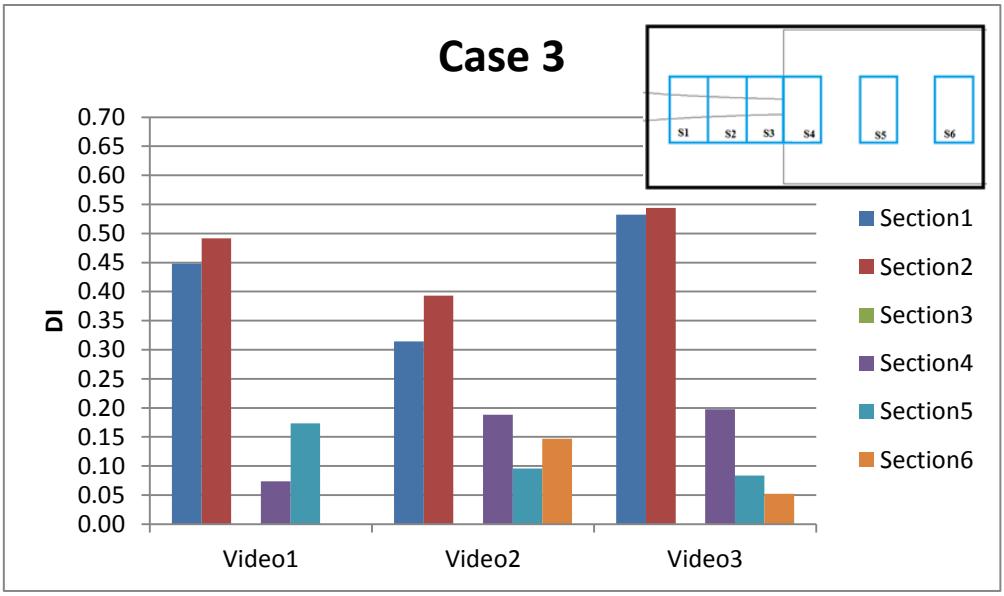

Figure 35: Comparison of DI for all videos in Case 3 in each section.

In this case it was observed the same problem as the previous cases. In the 3 videos the section 3 was missing. But the expected behaviour to the section 1, 2 and 3

was observed. In the video 1 the section 6 does not exist, too. Sections 4, 5 and 6 shows slightly different tendency among the 3 videos. However, this could be due to errors caused by the image quality.

Figure 36 shows the comparison between videos of case 4.

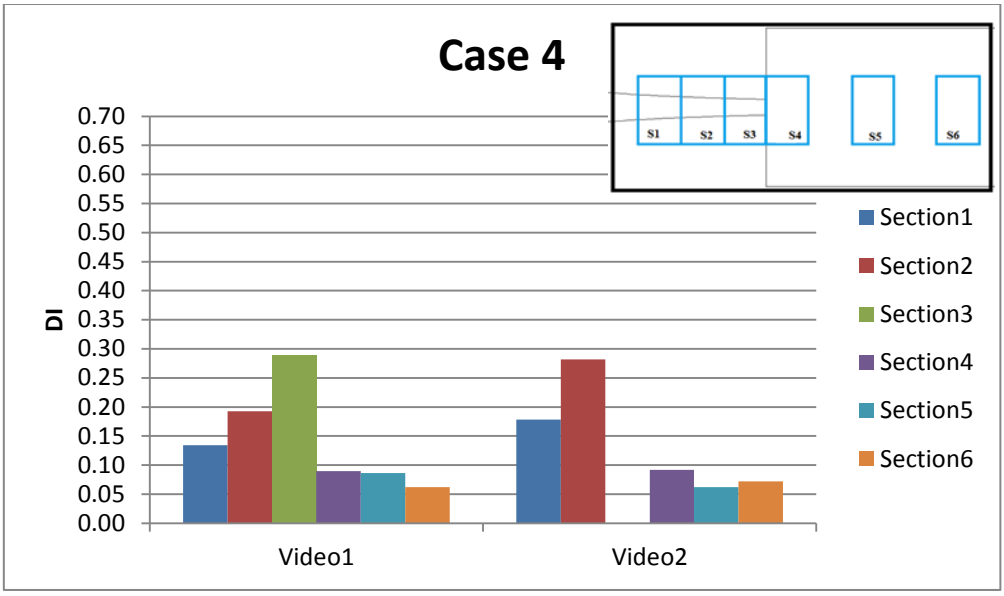

Figure 36: Comparison of DI for all videos in Case 4 in each section.

In this case 2 videos were obtained. Bode videos correspond well with the DI tendency observed in case 1, 2 and 3 but DI value is relatively lower. For instance, the maximum value in case 1 is about 0.55 whereas about 0.28 in case 4, and both values are from the same section 3.

Figure 37 shows the comparison between videos of case 5.

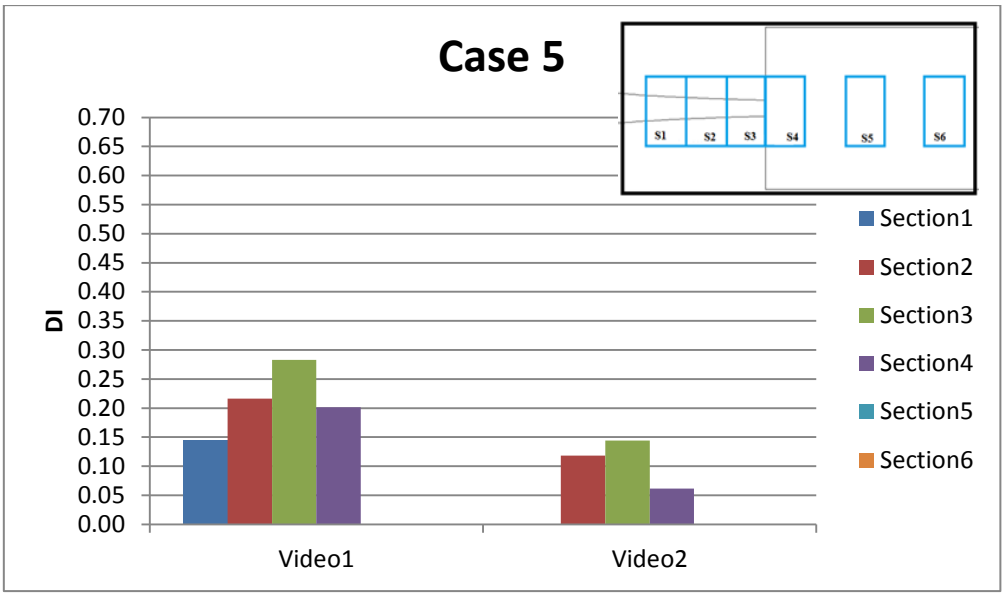

Figure 37: Comparison of DI for all videos in Case 5 in each section.

Once more, a lot of values are missing. For example, video 1 does not have section 5 and 6 and video 2 has only section 2, 3 and 4. Nevertheless, the graph shows similarity with case 5 and the maximum DI value was found in section 3.

Figure 38 gives the comparison between videos of case 6.

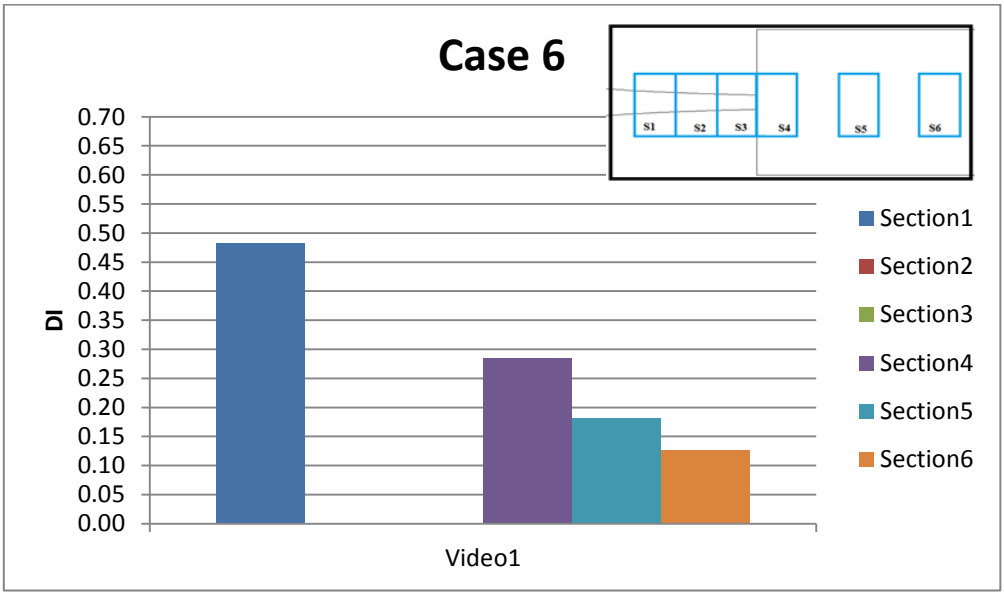

Figure 38: Comparison of the DI for all videos in Case 6 in each section.

In this case, only one video was obtained and was missing sections 2 and 3. Although it might not be relevant to observe, the graph shows a tendency that in sections 4 to 6 DI values are smaller than in section 1.

Figure 39 is the comparison between videos of case 7.

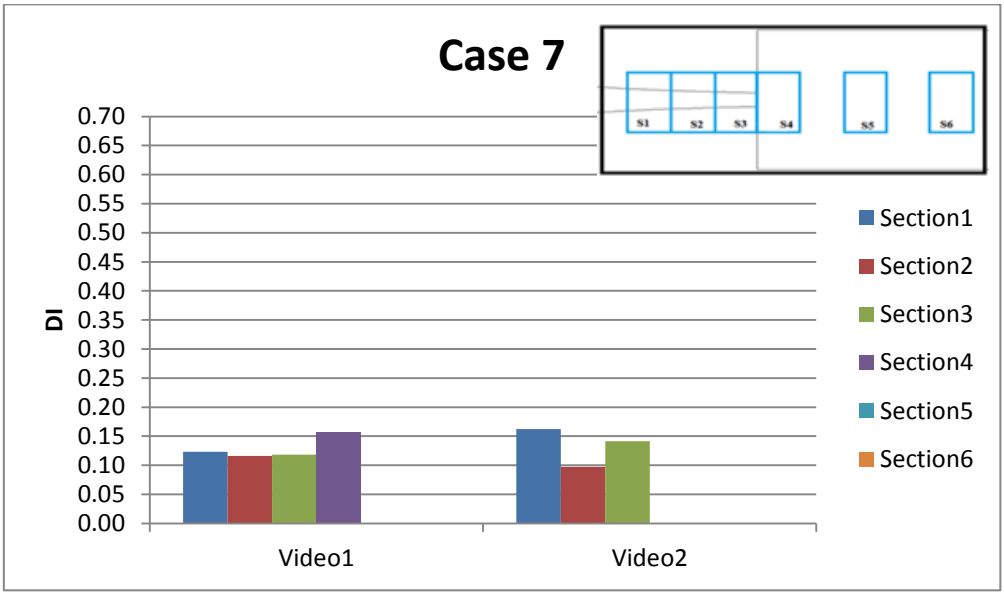

Figure 39: Comparison of DI for all videos in Case 7 in each section.

In this case, a lot of values are missing. The DI was not correspondent to the ideal behaviour seen in the other cases.

Figure 40 represents the average of all videos that were obtained for the cases 1, 4 and 5.

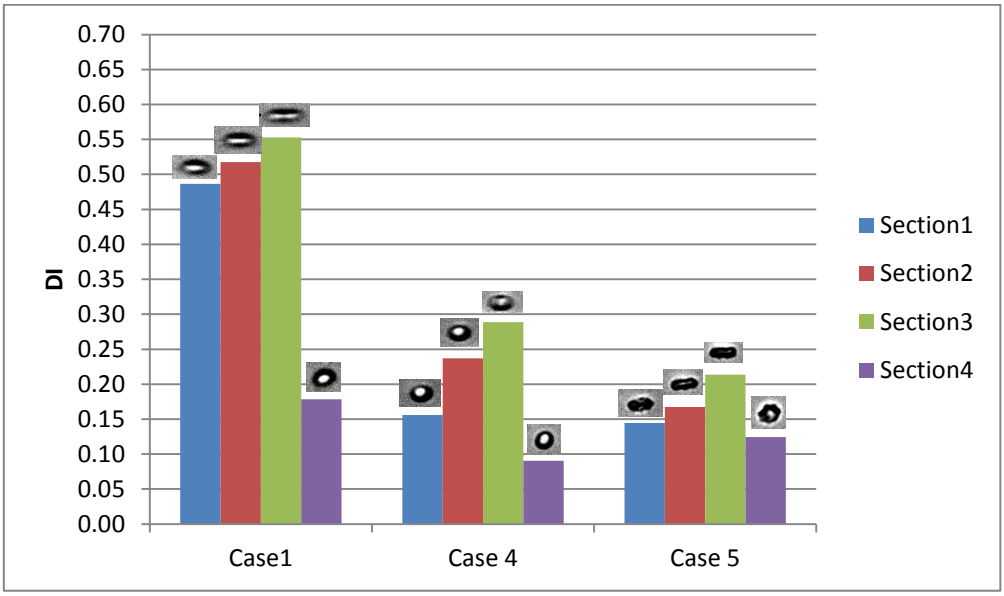

Figure 40: Comparison of average of DI to the cases 1, 4 and 5 for all videos.

As already have been shown, the results of image analysis include several lack of data due mainly to use of low Hct (2%) working fluids, and automatic measurement

method. Therefore, Case 1, 4 and 5 were used for comparison but Sections 5 and 6 were not compared due to lack of data.

By observing all the cases in the figure above, it is possible to say that DI increases from Section 1 to 3 and then at Section 4 DI dramatically decreases. The DI of Case 1 in Section 1, 2 and 3 are significantly higher than that of Case 4 and 5. The Case 1 is the erythrocytes that do not have contact with any tumour cell line whereas Case 4 and 5 are in contact with HCT15 for 24 hours and 48 hours respectively. Hence, it is possible to say that the healthy RBCs contacted with tumour cells for at least 24 hours get influence for their deformability, that is the increase of rigidity. In terms of DI comparison between Case 4 and 5, no significant difference is observed for all the sections. This could mean that the duration of time in contact with HCT - 15 for more than 24 hours is not an important influential factor for deformability of RBCs.

The current study has shown that for healthy erythrocytes a contact with tumour cells provides an influence, decreasing their deformability. However, to consolidate this result, further studies need to be conducted including high Hct environment and solid measurement methodologies.

3.2. Comparison between NCI-H460 and HCT15 cell lines

To evaluate if erythrocytes influence the growth of the cells, their growth inhibition was accessed by Sulforhodamine B colorimetric assay previously described. It was observed a decrease of 17.98% in the growth of HCT - 15 cells that were in contact with erythrocytes (Figure 41).

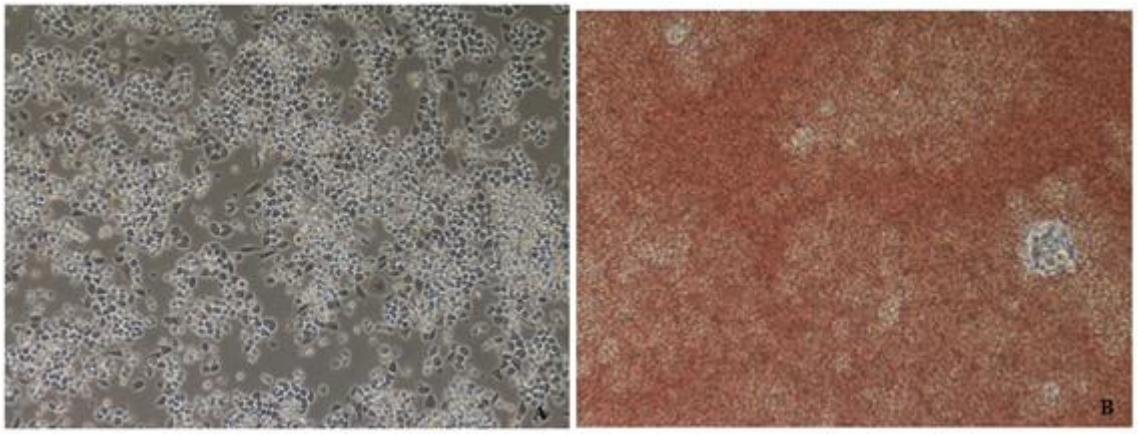

Figure 41: A - HCT15 cell line; B – HCT15 cell line with erythrocytes.

It was observed a decrease of 7.60% in the growth of NCI-H460 cells that were in contact with erythrocytes (Figure 42).

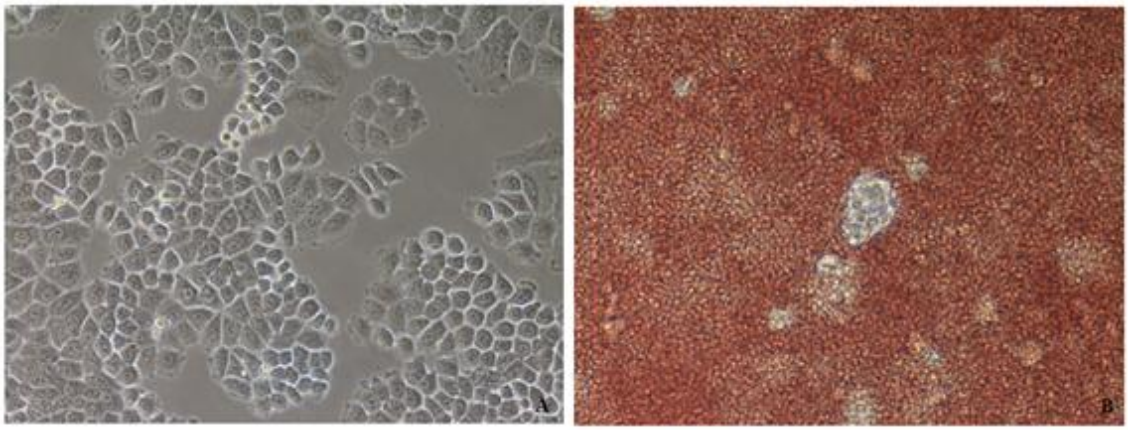

Figure 42: A –NCI-h460 cell line; B – NCI-H460 cell line with erythrocytes.

Overall, NCI-H460 cells proved to be less susceptible to erythrocytes presence than HCT15 cells.

4. Conclusions and Recommendations

In this study, erythrocytes deformability with a contact of tumor cells was examined using a hyperbolic microchannel. Despite several lack of data, there can be seen a tendency that the contact of tumor cells decrease deformation of RBCs. This was notably observed at the contraction part of the microchannel. The duration of time that tumor cells contact with healthy RBCs more than 24 hours did not show any significant differences. In order to confirm these results further studies are necessary with various conditions such as higher Hct.

Growth of tumor cells, NCI-H460 and HCT15, in contact with healthy RBCs was also examined. In both cases, their growth was suppressed but the NCI-H460 samples showed less susceptible presence than the HCT15 samples. Detailed investigation will be further needed including different concentration of tumor cells as well as RBCs for better understanding the reasons for this difference in growth of the cell lines.

References

Abbott, A.. (2003). Biology's new dimension. Nature, v. 424, p. 870-872.

Abkarian, M., Faivre, M., Horton, R., Smistrup, K., Best-Popescu, C. A. and Stone, H. A.. (2008). Cellular-scale hydrodynamics. Biomed. Mater., v. 3, 034011.

Anderson, J. R., Chiu, D. T., McDonald, J. C., Jackman, R. J., Cherniavskaya, O., Wu, H., Whitesides, S. and Whitesides, G. M.. (2000). Fabrication of topologically complex three-dimensional microfluidic systems in PDMS by rapid prototyping, Anal. Chem., v. 72, p. 3158–3164.

Angelo, R. W., Gelorme, J. D., Kuczynski, J. P., Lawrence, W. H., Pappas, S. P. and Simpson, L. L.. (1992). Photocurable epoxy composition with sulfonium salt photoinitiator. US Patent, 5102772.

Axisa, F., Brosteaux, D., De Leersnyder, E., Bossuyt, F., Vanfleteren, J., Hermans, B. and Puers, R.. (2007). Biomedical Stretchable Sytems using MID Based Stretchable Electronics Technology. In 12th International Conference of IEEE EMBS, France, pp. 5687-5690.

Baharvand, H., Hashemi, S. M., Ashtiani, S. K., Farrokhi, A.. (2006). Differentiation of human embryonic stem cells into hepatocytes in 2D and 3D culture system *in vitro*. Int. J. Dev. Biol., v. 50, p. 645–652.

Barker, S. L. R., Ross, D., Tarlov, M. J., Gaitan, M. and Locascio, L. E.. (2000). Control of flow direction in microfluidic devices with polyelectrolyte multilayers. Anal. Chem., v. 72, p. 5925-5929.

Battista, S., Guarnieri, D., Borselli, C., Zeppetelli, S., Borzacchiello, A., Mayol, L., Gerbasio, D., Keene, D. R., Ambrosio, L. and Netti, P. A.. (2005). The effect of matrix composition of 3D constructs on embryonic stem cell differentiation. Biomaterials, v. 26, p. 6194–6207.

Beachley, V. and Wen, X.. (2010). Polymer nanofibrous structures: Fabrication, biofunctionalization, and cell interactions. Progress in Polymer Science, v. 35, p. 868–892.

Beachley, V. and Wen, X.. (2009). Fabrication of nanofiber reinforced protein structures for tissue engineering. Mater. Sci. Eng. C., v. 29, p. 2448–2453.

Behravesh, E., Emami, K., Wu, H. and Gonda, S.. (2005). Comparison of genotoxic damage in monolayer cell cultures and three-dimensional tissue-like cell assemblies. Adv. Space Res., v. 35, p. 260-267.

Benya, P. D. and Shaffer, J. D.. (1982). Dedifferentiated chondrocytes re-express the differentiated collagen phenotype when cultured in agarose gels. Cell, v. 30, p. 215–224.

Berg, J. M., Anderson, R., Anaya, M., Lahlouh, B., Holtz, M. and Dallas, T.. (2003). A two-stage discrete peristaltic micropump. Sensors Actuators A, v. 104, p. 6-10.

Bertsch, A., Lorenz, H. and Renaud, P.. (1999). 3D microfabrication by combining microstereolithography and thick resist UV lithography. Sensors and Actuators A, v. 73, p. 14-23.

Bhattacharya, S., Datta, A., Berg, J. M. and Gangopadhyay, S.. (2005). Gangopadhyay, Studies on Surface Wettability of Poly(Dimethyl) Siloxane (PDMS) and Glass Under Oxygen-Plasma Treatment and Correlation With Bond Strength. J. MEMS, v. 14, p. 590-597.

Bianco, P. and Robey, P. G.. (2001). Stem cells in tissue engineering. Nature, v. 414, p. 118-121.

Birgersdotter, A., Sandberg, R. and Ernberg, I.. (2005). Gene expression perturbation *in vitro*—a growing case for three-dimensional (3D) culture systems. Semin. Cancer Biol., v. 15, p. 405-412.

Boey, S. K., Boal, D. H. and Discher, D. E.. (1998). Simulations of the erythrocyte cytoskeleton at large deformation. I. Microscopic models. Biophys. J., v. 75, p. 1573–1583.

Borselli, C., Oliviero, O., Battista, S., Ambrosio, L. and Netti, P. A.. (2007). Induction of directional sprouting angiogenesis by matrix gradients. J. Biomed. Mater. Res. A., v. 80, v. 297–305.

Buchko, C. J., Chen, L. C., Shen, Y. and Martin, D. C.. (1999). Processing and microstructural characterization of porous biocompatible protein polymer thin films. Polymer, v. 40, p. 7397–7407.

Burdick, J. A., Khademhosseini, A. and Langer, R. (2004). Fabrication of Gradient Hydrogels Using a Microfluidics/Photopolymerization Process. Langmuir, v. 20, p. 5153–5156.

Camps, J., About, I., Thonneman, B., Mitsiadis, T. A., Schmaltz, G. and Franquin, J. C.. (2002). Twoversus three-dimensional *in vitro* differentiation of human pulp cells into odontoblastic cells. Connect. Tissue Res., v. 43, p. 396-400.

Carlo, N. D. D., Wu, L. Y. and Lee, L. P.. (2006). Dynamic single cell culture array. Lab. Chip, v. 6, p. 1445–1449.

Caro, C., Pedley, T., Schroter, R. and Seed, W.. (1978). The mechanics of the circulation, Oxford University Press.

Charati, S. G. and Sterm, S.A.. (1998). Diffusion of gases in silicone polymers: molecular dynamic simulations, Macromolecules, v. 31, p. 5529–5535.

Chau, L. T., Rolfe, B. E. and Cooper-White, J. J.. (2011). A microdevice for the creation of patent, three-dimensional endothelial cell-based microcirculatory networks. Biomicrofluidics, v. 5, 034115.

Chaudhury, M. K. and Whitesides, G. M.. (1991). Direct measurement of interfacial interactions between semispherical lenses and flat sheets of poly(dimethylsiloxane) and their chemical derivatives. Langmuir, v. 7, p. 1013-1025.

Cho, Y. I., Mooney, M. P. and Cho, D. J.. (2008). Hemorheologiccal disorders in diabetes mellitus. Journal of diabetes science and technology, v. 2, p. 1130-1138.

Cima, L. G., Vacanti, J. P., Vacanti, C., Ingber, D., Mooney, D., and Langer, R.. (1991). Tissue engineering by cell transplantation using biodegradable polymer substrates. J. Biomech. Eng., v.113, p. 143-151.

Cukierman, E., Pankov, R., Stevens, D. R. and Yamada, K. M.. (2001). Taking cell–matrix adhesions to the third dimension. Science, v. 294, p. 1708–1712.

Data recovery, http://www.datarecovery.com/clean.asp - accessed on June 2012.

Day, R. M., Boccaccini, A. R., Maquet, V., Shurey, S., Forbes, A., Gabe, S. M. and Jerome, R.. (2004). In vivo characterisation of a novel bioresorbable poly(lactideco-glycolide) tubular foam scaffold for tissue engineering applications. J. Mater. Sci. Mater. Med., v. 15, p. 729–734.

Deitzel, J. M., Kleinmeyer, J., Hirvonen, J. K. and Beck, T. N. C.. (2001). Controlled deposition of electrospun poly(ethylene oxide) fibers. Polymer, v. 42, p. 8163–8170.

DiMilla, P. A., Barbee, K. and Lauffenburger, D. A.. (1991). Mathematical model for the effects of adhesion and mechanics on cell migration speed. Biophys. J., v. 60, p. 15-37.

Discher, D. E., Mohandas, N. and Evans, E. A.. (1994). Molecular maps of red-cell deformation: hidden elasticity and in situ connectivity. Science, v. 266, p. 1032–1035.

Discover Magazine, http://blogs.discovermagazine.com/80beats/2010/11/08/going-direct-researchers-change-skin-into-blood-with-no-stops-in-between/ - Accessed on 10 July 2012

Doshi, J., and Reneker, D. H.. (1995). Electrospinning process and applications of electrospun fibers. J. Electrostatics, v. 35, p.151–160.

Duffy, D. C., McDonald, J. C., Schueller, O. J. A. and Whitesides, G.M.. (1998). Rapid Prototyping of Microfluidic Systems in Poly(dimethylsiloxane). Anal. Chem., v. 70, p. 4974-4984.

Efimenko, K., Wallace, W. E. and Genzer, J.. (2002). Surface modification of Sylgard-184 poly(dimethyl siloxane) networks by ultraviolet and ultraviolet/ozone treatment. J. Colloid. Interface Sci., v. 254, p. 306-315.

Eichhorn, S. J. and Sampson, W. W.. (2005). Statistical geometry of pores and statistics of porous nanofibrous assemblies. J. R. Soc. Interface, v. 2, p. 309–318.

El Haj, A. J., Wood, M. A., Thomas, P. and YingYang.. (2005). Controlling cell biomechanics in orthopaedic tissue engineering and repair. Pathologie Biologie, v. 53, p. 581–589.

El-Ali, J., Sorger, P. K. and Jensen, K. F.. (2006). Cells on chips. Nature, v. 442, p. 403-411.

Entschladen, F., Drell IV, T. L., Lang, K., Masur, K., Palm, D., Bastian, P., Niggemann, B. and Zaenker, K. S.. (2005). Analysis methods of human cell migration. Experimental Cell Research, v. 307, p. 418 – 426.

Erdodi, G. and Kennedy, J. P.. (2005). Water-swollen higly oxygen permeable membranes: analytical technique and syntheses. Journal of Polymer Science: Part A: Polymer Chemistry, v. 43, p. 3491-3501.

Evans, E. A. and La Celle, P. L.. (1975). Intrinsic material properties of erythrocyte membrane indicated by mechanical analysis of deformation. Blood, v. 45, p. 29–43

Evans, E. A.. (1973). New membrane concept applied to the analysis of fluid shear- and micropipette-deformed red blood cells. Biophys. J., v. 13, p. 941–954

Faivre, M., Abkarian, M., Bickraj, K. and Stone, H.. (2006). Geometrical focusing of cells in a microfluidic device: An approach to separate blood plasma. Biorheology, v. 43, p. 147.

Fertala, A., Han, W. B. and Ko, F. K.. (2001). Mapping critical sites in collagen II for rational design of gene-engineered proteins for cell-supporting materials. J. Biomed. Mater. Res., v. 57, p. 48–58.

Fiorini, G. S. and Chiu, D. T.. (2005). Disposable microfluidic devices: fabrication, function, and application. BioTechniques, v. 38, p. 429-446.

Fong, H. and Reneker, D. H.. (2001). Electrospinning and formation of nanofibers. In: Salem DR, editor. Structure formation in polymeric fibers. Munich: Hanser;. p. 225–246.

Friedl, P. and Brocker, E. B.. (2000). The biology of cell locomotion within three-dimensional extracellular matrix. Cell Mol. Life Sci., v. 57, p. 41-64.

Friedl, P. and Wolf, K.. (2003). Tumour-cell invasion and migration: diversity and escape mechanisms. Nat. Rev. Cancer, v. 3, p. 362-374.

Fujiwara, H., Ishikawa, T., Lima, R., Matsuki, N., Imai, Y., Kaji, H., Nishizawa, M. and Yamaguchi, T.. (2009). Red blood cell motions in high-hematocrit blood flowing through a stenosed microchannel. J. Biomech., v. 42, p. 838.

Galletti, P. M., Hellman, K. B. and Nerem, R. M.. (1995). Tissue engineering: from basic science to products: a preface. Tissue Eng. Summer, v. 1, p. 147-149.

Garcia, V., Dias, R. and Lima, R. (2012). Applied Biological Engineering – Principles and Practice, Chapter 17 - In Vitro Blood Flow Behaviour in Microchannels with Simple and Complex Geometries.

Geiger, B., Spatz, J. P. and Bershadsky, A. D.. (2009). Environmental sensing through focal adhesions. Nat. Rev. Mol. Cell Biol., v. 10, p. 21–33.

Gibson, P. W., Schreuder-Gibson, H. L., Riven, D.. (1999). Electrospun fiber mats: transport properties. AIChE. J., v. 45, p. 190–195.

Gilbert, S. F.. (2003). The morphogenesis of evolutionary developmental biology. Int. J. Dev. Biol., v. 47, p. 467–477.

Gillmor, S. D., Larsen, B. J., Braun, J. M., Mason, C. E., Cruz-Barba, L. E., Denes, F. and Lagally, M. G.. (2002). In Proceedings of the Second Annual International IEEE-EMBS

Special Topic Conference on Microtechnologies in Medicine and Biology, IEEE xplore: Wisconsin-Madison, USA, p. 51.

Griffith, L. G., and Naughton, G.. (2002). Tissue Engineering: Current Challenges and Expanding Opportunities. Science, v. 295, p. 1009–1014.

Grover, W. H., Ivester, R. H., Jensen, E. C. and Mathies, R. A.. (2006). Development and multiplexed control of latching pneumatic valves using microfluidic logical structures. Lab. Chip, v. 6, p. 623-631.

Grzybowski, B. A., Haag, R., Bowden, N. and Whitesides, G. M.. (1998). Generation of micrometer sized patterns for microanalytical applications using a laser direct-Write method and microcontact printing. Anal. Chem., v. 70, p. 4645-4652.

Hanahan, D. and Weinberg, R. A.. (2000). The hallmarks of cancer. Cell, v. 100, p. 57-70.

Hardeman, M. R. and Ince, C.. (1999). Clinical potencial of *in vitro* measured red cell deformability, a myth?. Clinical Hemorheology and Microcirculation, v. 21, p. 277-284.

Hemmrich, K. and von Heimburg, D.. (2006). Biomaterials for adipose tissue engineering. Expert Rev. Med. Devices, v.3, p. 635-645.

Hongbin, Y., Guangya, Z., Siong, C. F., Shouhua, W. and Feiwen, L.. (2009). Novel polydimethylsiloxane (PDMS) based microchannel fabrication method for lab-on-a-chip application. Sens. Actuators B, v. 137, p. 754-761.

Horwitz, R. and Webb, D.. (2003). Cell migration. Current Biology, v. 13, p. 756-759.

Hou, H. W., Han, J., and Lim, C. T.. (2010). Deformability based cell margination – A simple microfluidic design for malaria infected erythrocyte separation. Lab. Chip, v. 10, p. 2605-2613.

Hu, G., Quaranta, V. and Li, D.. (2007). Modeling of effects of nutrient gradients on cell proliferation in microfluidic bioreactor. Biotechnol. Prog., v. 23, p. 1347-1354.

Hu, S., Ren, X., Bachman, M., Sims, C. E., Li, G. P. and Allbritton, N.. (2002). Surface Modification of Poly(dimethylsiloxane) Microfluidic Devices by Ultraviolet Polymer Grafting. Anal. Chem., v. 74, p. 4117-4123.

Huang, Z. M., Zhang, Y.-Z., Kotaki, M. and Ramakrishna, S.. (2003). A review on polymer nanofibers by electrospinning and their applications in nanocomposites. Composites Science and Technology, v. 63, p. 2223–2253.

Hudon, V., Berthod, F., Black, A. F., Damour, O., Germain, L. and Auger, F. A.. (2003). A tissue-engineered endothelialized dermis to study the modulation of angiogenic and angiostatic molecules on capillary-like tube formation in vitro. Br. J. Dermatol., v. 148, p. 1094–1104.

Ito, A., Mase, A., Takizawa, Y., Shinkai, M., Honda, H., Hata, K., Ueda, M. and Kobayashi, T.. (2003). Transglutaminase-mediated gelatin matrices incorporating cell adhesion factors as a biomaterial for tissue engineering. J. Biosci. Bioeng., v. 95, v. 196–199.

Jaeger, C. J.. (2002). Introduction to microelectronic fabrication. New Jersy: Prentice Hall.

Jeon, N. L., Chiu, D. T., Wargo, C. J., Wu, H. K., Choi, I. S., Anderson, J. R. and Whitesides, G. M.. (2002). Design and fabrication of integrated passive valves and pumps for flexible polymer 3-dimensional microfluidic systems. Biomed. Microdevices, v. 4, p. 117-121.

Jeon, O., Ryu, S.H., Chung, J.H. and Kim, B.S.. (2005). Control of basic fibroblast growth factor release from fibrin gel with heparin and concentrations of fibrinogen and thrombin. J. Control Release, v. 105, p. 249–259.

Jin, H. J., Fridrikh, S., Rutledge, G. C., Kaplan, D.. (2002). Electrospinning Bombyx mori silkwith poly(ethylene oxide). Abstracts of Papers American Chemical Society, v. 224, p. 408.

Kane, R. S., Takayama, S., Ostuni, E., Ingber, D. E. and Whitesides, G. M.. (1999). Patterning proteins and cells using soft lithography. Biomaterials, v. 20, p. 2363–2376.

Kapur, T. A. and Shoichet, M. S.. (2004). Immobilized concentration gradients of nerve growth factor guide neurite outgrowth. J. Biomed. Mater. Res. A., v. 68, p. 235–243.

Khademhosseini, A., Langer, R., Borenstein, J., and Vacanti, J. P.. (2005). Microscale technologies for tissue engineering and biology. PNAS, vol. 103, p. 2480–2487.

Kollet, O., Shivtiel, S., Chen, Y. Q., Suriawinata, J., Thung, S. N., Dabeva, M. D., Kahn, J., Spiegel, A., Dar, A., Samira, S., Goichberg, P., Kalinkovich, A., Arenzana-Seisdedos, F., Nagler, A., Hardan, I., Revel, M., Shafritz, D. A. and Lapidot, T.. (2003). HGF, SDF-1, and MMP-9 are involved in stress-induced human CD34+ stem cell recruitment to the liver. J. Clin. Invest., v. 112, p. 160– 169.

Lacour, S. P., Tsay, C. and Wagner, S.. (2004). An elastically stretchable TFT circuit. IEEE Electron Device Letter, v. 25, p. 792-794.

Langer, R. and Tirrell, D. A.. (2004). Designing materials for biology and medicine. Nature, v. 428, p. 487–492.

Langer, R., and Vacanti, J. P.. (1993). Tissue engineering. Science, v. 260, p. 920–926.

Lannutti, J., Reneker, D., Ma, T., Tomasko, D. and Farson, D.. (2007). Electrospinning for tissue engineering scaffolds. Mater. Sci. Eng. C. Biomimetic. Supramol. Syst., v. 27, p. 504–509.

Lanza, R., Langer, R. and Vacanti, J. P.. (2000). Principles of tissue engineering: Academic Press, 2nd edition.

Lee, J. E., Kim, S. E., Kwon, I. C., Ahn, H. J., Cho, H., Lee, S. H., Kim, H. J., Seong, S. C. and Lee, M. C.. (2004). Effects of a chitosan scaffold containing TGF-beta1 encapsulated chitosan microspheres on in vitro chondrocyte culture. Artif. Organs., v. 28, p. 829–839.

Lee, K. Y., LaBianca, N., Rishton, S. A., Zolghamain, S., Gelorme, J. D., Shaw, J. and Chang, H. P.. (1995). Micromachining applications of a high resolution ultrathick photoresist. J. Vac. Sci. Technol. B., v. 13, p. 3012-3016.

LeGeros, R.Z.. (2002). Properties of osteoconductive biomaterials: calcium phosphates. Clin. Orthop. Relat Res., p. 81–98.

Levenberg, S., and Langer, R.. (2004). Chapter 5 - Advances in Tissue Engineering. Current Topics in Developmental Biology, v. 61, p. 113-135.

Levenberg, S., Huang, N. F., Lavik, E., Rogers, A. B., Itskovitz-Eldor, J. and Langer, R.. (2003). Differentiation of human embryonic stem cells on three-dimensional polymer scaffolds. Proc. Natl. Acad. Sci. U.S.A., v. 100, p. 12741-12746.

Li, N., Tourovskaia, A. and Folch, A.. (2003). Biology on a Chip: Microfabrication for Studying the Behaviour of Cultured Cells. Critical Reviews™ in Biomedical Engineering, v. 31, p. 423–488.

Lima, R., Fernandes, C. S., Dias, R. P., Ishikawa, T., Imai, Y.: T. Yamaguchi, in Computational Vision and Medical Image Processing: Recent Trends, edited by J. M. R. S. Tavares and R. M. N. Jorge (Springer Science+Business Media B.V., Netherlands, 2011), p. 297.

Linder, V., Verpoorte, E., Thormann, W., de Rooji, N. F. and Sigrist, H.. (2001). Surface biopassivation of replicated poly(dimethylsiloxane) microfluidic channels and application to heterogeneous immunoreaction with on-chip fluorescence detection. Anal. Chem., v. 73, p. 4181-4189.

Liu, Y., Fanguy, J. C., Bledsoe, J. M. and Henry, C. S.. (2000). Dynamic coating using polyelectrolyte multilayers for chemical control of electroosmotic flow in capillary electrophoresis microchips. Anal. Chem., v. 72, p. 5939-5944.

Liu, Y., Yang, D., Yu, T. and Jiang, X.. (2009). Incorporation of electrospun nanofibers PVDF membranes into a microfluidic chip assembled by PDMS and scotch tape for immunoassays. Electrophoresis, v. 30, p. 3269-3275.

Lutolf, M. P. and Hubbell, J. A.. (2005). Synthetic biomaterials as instructive extracellular microenvironments for morphogenesis in tissue engineering. Nat. Biotechnol., v. 23, p. 47–55.

Lutolf, M. P., Lauer-Fields, J. L., Schmoekel, H. G., Metters, A. T., Weber, F. E., Fields, G.B. and Hubbell, J.A.. (2003). Synthetic matrix metalloproteinasesensitive hydrogels for the conduction of tissue regeneration: engineering cell-invasion characteristics. Proc. Natl. Acad. Sci. U. S. A., v. 100, p. 5413–5418.

Ma, Z., Kotaki, M., Inai, R. and Ramakrishna, S.. (2005). Potential of nanofiber matrix as tissue-engineering scaffolds. Tissue Eng., v. 11, p. 101–109.

Madou, M. J. (2002.). Fundamentals of microfabrication: the science of miniaturization edn 2nd. Boca Raton, Florida, CRC Press LLC.

Maji, D., Lahirib, S. K. and Das, S.. (2012). Study of hydrophilicity and stability of chemically modified PDMS surface using piranha and KOH solution. Surf. Interface Anal., v. 44, p. 62–69.

Makamba, H., Kim, J. H., Lim, K., Park, N. and Hahn, J. H.. (2003). Surface modification of poly(dimethylsiloxane) microchannels. Electrophoresis, v. 24, p. 3607–3619.

Malafaya, P. B., Silva, G. A. and Reis, R. L.. (2007). Natural-origin polymers as carriers and scaffolds for biomolecules and cell delivery in tissue engineering applications. Adv. Drug Deliv. Rev., v. 59, p. 207–233.

Mann, B. K., Schmedlen, R. H. and West, J. L.. (2001). Tethered-TGF-beta increases extracellular matrix production of vascular smooth muscle cells. Biomaterials, v. 22, p. 439-444.

Mansbridge, J., Liu, K., Patch, R., Symons, K. and Pinney, E.. (1998). Three-dimensional fibroblast culture implant for the treatment of diabetic foot ulcers: metabolic activity and therapeutic range. Tissue Eng., v. 4, p. 403-414.

Martin, I., Suetterlin, R., Baschong, W., Heberer, M., Vunjak-Novakovic, G. and Freed, L. E.. (2001). Enhanced cartilage tissue engineering by sequential exposure of chondrocytes to FGF-2 during 2D expansion and BMP-2 during 3D cultivation. J. Cell Biochem., v. 83, p. 121-128.

Masson, S., Harrison, D. J., Plevris, J. N. and Newsome, P. N.. (2004). Potential of hematopoietic stem cell therapy in hepatology: a critical review. Stem. Cells, v. 22, p. 897– 907.

Mata, A., Fleischmann, A. J. and Roy, S.. (2005). Characterization of polydimethylsiloxane (PDMS) properties for biomedical micro/nanosystems. Biomed. Microdevices, v. 7, p. 281-293.

Mazo, M., Planat-Bénard, V., Abizanda, G., Pelacho, B., Léobon, B., Gavira, J. J., Peñuelas, I., Cemborain, A., Pénicaud, L., Laharrague, P., Joffre, C., Boisson, M., Ecay, M., Collantes, M., Barba, J., Casteilla, L. and Prósper, F.. (2008). Transplantation of adipose derived stromal cells is associated with functional improvement in a rat model of chronic myocardial infarction. European Journal of Heart Failure, v. 10, p. 454–462.

McDonald, J. C. and Whitesides, G. M.. (2002). Poly(dimethylsiloxane) as a material for fabricating microfluidic devices. Acc. Chem. Res., v. 35, p. 491-499.

McDonald, J. C., Duffy, D. C., Anderson, J. R., Chiu, D. T., Wu, H., Schueller, O. J. and Whitesides, G. M.. (2000). Fabrication of microfluidic systems in poly(dimethylsiloxane). Electrophoresis, v. 21, p. 27-40.

Meng, J., Kong, H., Han, Z., Wang, C., Zhu, G., Xie, S. and Xu, H.. (2009). Enhancement of nanofibrous scaffold of multiwalled carbon nanotubes/ polyurethane composite to the fibroblasts growth and biosynthesis. J. Biomed. Mater. Res. A., v. 88, p. 105–116.

Mohandas, N. and Chasis, J. A.. (1993). Red blood cell deformability, membrane material properties and shape: regulation by transmembrane, skeletal and cytosolic proteins and lipids. Semin. Hematol., v. 30, p.171–192.

Mohandas, N. and Evans, E. A.. (1994). Mechanical properties of the red cell membrane in relation to molecular structure and genetic defects. Ann. Rev. Biophys. Biomol. Struct., v. 23, p. 787–818.

Morent, R., De Geyter, N., Axisa, F., De Smet, N., Gengembre, L., De Leersnyder, E., Leys, C., Vanfleteren, J., Rymarczyk-Machal, M., Schacht, E. and Payen, E.. (2007). Adhesion enhancement by a dielectric barrier discharge of PDMS used for flexible and stretchable electronics. J. Phys. D: Appl. Phys., v. 40, p. 7392.

Moser, B., Wolf, M., Walz, A. and Loetscher, P.. (2004). Chemokines: multiple levels of leukocyte migration control. Trends Immunol., v. 25, p. 75–84.

Mueller-Klieser, W.. (1997). Three-dimensional cell cultures: from molecular mechanisms to clinical applications. Am. J. Physiol., v. 273, p. C1109-1123.

Musielak, M.. (2009). Red blood cell-deformability measurement: review of techniques. Clinical Hemorheology and microcirculation, v. 42, p. 47-64.

Nakano, A., Sugii, Y., Minamiyama, M., Seki, J. and Niimi, H.. (2005). Velocity profiles of pulsatile blood flow in arterioles with bifurcation and confluence in rat mesnetery measured by particle image velocimetry. JSME Int. J., Ser. C, v. 48, p. 444-452.

Nakano, T., Itoyama, T., Yoshida, K., Sawada, Y., Ikeda, S., Fukuda, T., Matsuda, T., Negoro, M. and Arai, F.. (2010). Multiscale fabrication of a transparent circulation type blood vessel simulator. Biomicrofluidics, v. 4, 046505.

Nerem, R. M.. (1991). Cellular engineering. Ann. Biomed. Eng., v. 19, p. 529–545.

Ng, K. W., Hutmacher, D. W., Schantz, J. T., Ng, C. S., Too, H. P., Lim, T. C., Phan, T. T. and Teoh, S. H.. (2001). Evaluation of ultra-thin poly(epsilon-caprolactone) films for tissue-engineered skin. Tissue Eng., v. 7, p. 441–455.

Niea, F-Q., Yamadaa, M., Kobayashia, J., Yamatoa, M., Kikuchia, A. and Okanoa, T.. (2007). On-chip cell migration assay using microfluidic channels. Biomaterials, v. 28, p. 4017–4022.

Ogawa, R. (2006). The importance of adipose-derived stem cells and vascularized tissue regeneration in the field of tissue transplantation. Curr. Stem Cell Res. Ther., v. 1, p. 13-20.

Okamoto, T., Yamamoto, Y., Gotoh, M., Huang, C. L, Nakamura, T., Shimizu, Y., Tabata, Y. and Yokomise, H.. (2004). Slow release of bone morphogenetic protein 2 from a gelatin sponge to promote regeneration of tracheal cartilage in a canine model. J. Thorac. Cardiovasc. Surg., v. 127, p. 329–334.

Ostuni, E., Chen, C.S., Ingber, D.E. and Whitesides, G.M.. (2001). Selective deposition of proteins and cells in arrays of microwells. Langmuir v. 17, p. 2828-2834.

Ostuni, E., Yan, L. and Whitesides, G. M.. (1999). The interaction of proteins and cells with self-assembled monolayers of alkanethiolates on gold and silver. Colloids Surf. B Biointerfaces, v. 15, p. 3–30.

Pachence, J. M.. (1996). Collagen-based devices for soft tissue repair. J. Biomed. Mater. Res., v. 33, v. 35–40.

Palecek, S. P., Loftus, J. C., Ginsberg, M. H., Lauffenburger, D. A. and Horwitz, A. F.. (1997). Integrin-ligand binding properties govern cell migration speed through cell-substratum adhesiveness. Nature, v. 385, p. 537-540.

Pardon, J. M., Van der Wilt, C. L., Smid, K., Smitskamp-Wilms, E., Baukus, H. H., Piazo, P. E., Giaccone, G., Peters, G. J.. (2000). The multilayered postconfluent cell culture as a model for drug screening. Crit. Rev. Oncol. Hematol, v. 36, p. 147–157.

Paul, W. and Sharma, C.P.. (2003). Ceramic drug delivery: a perspective. J. Biomater. Appl., v. 17, p. 253–264.

Perets, A., Baruch, Y., Weisbuch, F., Shoshany, G., Neufeld, G. and Cohen, S.. (2003). Enhancing the vascularization of three-dimensional porous alginate scaffolds by incorporating controlled release basic fibroblast growth factor microspheres. J. Biomed. Mater. Res. A., v. 65, p. 489–497.

Petrie, R. J., Doyle, A. D. and Yamada, K. M.. (2009). Random versus directionally persistent cell migration. Nat. Rev. Mol. Cell Biol., v. 10, p. 538–549.

Pham, Q. P., Sharma, U., and Mikos, A. G.. (2006). Electrospinning of Polymeric Nanofibers for Tissue Engineering Applications: A Review. Tissue Engineering, v. 12, p. 1197-1211.

Prokop, A., Prokop, Z., Schaffer, D., Kozlov, E., Wikswo, J.P., Cliffel, D. and Baudenbacher, F.. (2004). NanoLiterBioReactor: Monitoring of Long-Term Mammalian Cell Physiology at Nanofabricated Scale. Biomedical Microdevices, v. 6, p. 325-339.

Provenzano, P.P., Inman, D. R., Eliceiri, K. W., Trier, S. M. and Keely, P. J.. (2008). Contact Guidance Mediated Three-Dimensional Cell Migration is Regulated by Rho/ROCK-Dependent Matrix Reorganization. Biophys J., v. 95, p. 5374–5384.

Rahbari, R., Sheahan, T., Modes, V., Collier, P., Macfarlane, C. and Badge, R. M.. (2009). A novel L1 retrotransposon marker for HeLa cell line identification. BioTechniques, v. 46, p. 277–284.

Reddi, A. H.. (1998). Role of morphogenetic proteins in skeletal tissue engineering and regeneration. Nat. Biotechnol., v. 16, p. 247-252.

Rikitake, Y. and Takai, Y.. (2011). Directional Cell Migration: Regulation by Small G Proteins, Nectin-like Molecule-5, and Afadin. Int. R. Cell and Mol. Biol., v. 287, p. 97-143.

Ryan, J. A.. (2008). Introdution to animal cell culture, technical Bulletin. Corning incorporated, New York, p. 1-7.

Sanghavi, J. N., Rabe, K. F., Kim, J. S., Magnussen, H., Leff, A. R. and White, S. R.. (1994). Migration of human and guinea pig airway epithelial cells in response to calcitonin gene-related peptide. Am. J. Respir. Cell Mol. Biol., v. 11, p. 181–187.

Scherer, W. F., Syverton, J. T. and Gey, G. O.. (1953). Studies on the propagation *in vitro* of poliomyelitis viruses. IV. Viral multiplication in a stable strain of human malignant epithelial cells (strain HeLa) derived from an epidermoid carcinoma of the cervix. J. Exp. Med., v. 97, p. 695–710.

Schnell, E., Klinkhammer, K., Balzer, S., Brook, G., Klee, D., Dalton, P. and Mey, J.. (2007). Guidance of glial cell migration and axonal growth on electrospun nanofibers of poly-epsilon-caprolactone and a collagen/poly-epsilon-caprolactone blend. Biomaterials, v. 28, p. 3012–3025.

Segura, T., Anderson, B. C., Chung, P. H., Webber, R. E., Shull, K. R. and Shea, L.D.. (2005). Crosslinked hyaluronic acid hydrogels: a strategy to functionalize and pattern Biomaterials, v. 26, p. 359–371.

Shevkoplyas, S. S., Yoshida, T., Gifford, S. C. and Bitensky, M. W.. (2006). Direct measurement of the impact of impaired erythrocyte deformability on microvascular network perfusion in a microfluidic device. Lab Chip, v. 6, p. 914-920.

Shevkoplyas, S. S., Yoshida, T., Munn, L. L. and Bitensky, M. W.. (2005). Biomimetic autoseparation of leukocytes from whole blood in a microfluidic device. Anal. Chem., v. 77, p. 933-937.

Shi, C., Zhu, Y., Ran, X., Wang, M., Su, Y. and Cheng, T.. (2006). Therapeutic potential of chitosan and its derivatives in regenerative medicine. J. Surg. Res., v. 133, v. 185–192.

Shin, S., Ku, Y., Ho, J., Kim, Y., Suh, J. and Singh, M.. (2007). Progressive impairment of erythrocyte deformability as indicator of microangiopathy in type 2 diabetes mellitus. Clinical hemorheology and microcirculation, v. 36, p. 253-261.

Sia, S. K. and Whitesides, G. M.. (2003). Microfluidic devices fabricated in poly(dimethylsiloxane) for biological studies. Electrophoresis, v. 24, p. 3563-3576.

Singer, A.J. and Clark, R. A.. (1999). Cutaneous wound healing. N. Engl. J. Med., v. 341, p. 738–746.

Sokolsky-Papkov, M., Agashi, K., Olaye, A., Shakesheff, K. and Domb, A. J.. (2007). Polymer carriers for drug delivery in tissue engineering. Adv. Drug Deliv. Rev., v. 59, p. 187–206.

Stark, H. J., Boehnke, K., Mirancea, N., Willhauck, M. J., Pavesio, A., Fusenig, N. E. and Boukamp, P.. (2006). Epidermal homeostasis in long-term scaffoldenforced skin equivalents. J. Investig. Dermatol. Symp. Proc., p. 93–105.

Sterodimas, A., Jose de Faria, Nicaretta, B. and Pitanguy, I.. (2010). Tissue engineering with adipose-derived stem cells (ADSCs): Current and future applications. Journal of Plastic, Reconstructive & Aesthetic Surgery, v. 63, p. 1886-1892.

Swindle, C. S., Tran, K. T., Johnson, T. D., Banerjee, P., Mayes, A. M., Griffith, L. and Wells, A.. (2001). Epidermal growth factor (EGF)-like repeats of human tenascin-C as ligands for EGF receptor. J. Cell Biol., v. 154, p. 459-468.

Thorsen, T., Maerkl, S. J. and Quake, S. R.. (2002). Microfluidic large-scale integration. Science, v. 298, p. 580-584.

Toepke, M. W. and Beebe, D. J.. (2006). PDMS absorption of small molecules and consequences in microfluidic applications. Lab Chip., v. 6, p. 1484–1486.

Tourovskaia, A., Figueroa-Masot, X. and Folch, A.. (2004). Differentiation-on-a-chip: A microfluidic platform for long-term cell culture studies. Lab Chip, v. 5, p. 14-19.

Tsukada, K., Sekizuka, E., Oshio, C. and Minamitani, H.. (2001). Direct measurement of Erythrocyte deformability in diabetes Mellitus with a transparente microchannel capillary model and high-speed vídeo cameta system. Micr. research, v. 61, p. 231-239.

Tysseling-Mattiace, V .M., Sahni, V., Niece, K. L., Birch, D., Czeisler, C., Fehlings, M. G., Stupp, S. I. and Kessler, J. A.. (2008). Self-assembling nanofibers inhibit glial scar formation and promote axon elongation after spinal cord injury. J. Neurosci., v. 28, p. 3814–3823.

Vasita, R. and Katti, D. S.. (2006). Nanofibers and their applications in tissue engineering. Int. J. Nanomed., v. 1, p. 15–30.

Veleva, A. N., Heath, D. E., Johnson, J. K., Nam, J., Patterson, C., Lannutti, J. J. and Cooper, S. L.. (2008). Interactions between endothelial cells and electrospun methacrylic terpolymer fibers for engineered vascular replacements. J. Biom. Mat. R. A, p. 1132-1139.

Venugopal, J., Low, S., Choon, A. T. and Ramakrishna, S.. (2008). Interaction of cells and nanofiber scaffolds in tissue engineering. J. Biomed. Mater. Res. B Appl. Biomater., v. 84, p. 34–48.

Vickers, J. A., Caulum, M. M. and Henry, C. S.. (2006). Generation of Hydrophilic Poly(dimethylsiloxane) for High-Performance Microchip Electrophoresis. Anal. Chem., v. 78, p. 7446-7452.

Walker, G. M., Zeringue, H. C. and Beebe, D. J.. (2004). Microenvironment design considerations for cellular scale studies. Lab Chip, v. 4, p. 91-97.

Whitesides, G. M., Ostuni, E., Takayama, S., Jiang, X. and Ingber, D.E.. (2001). Soft lithography in Biology and Biochemistry. Ann. Rev. Biomed. Eng. V. 3, p. 335-373.

Wolf, K., Mazo, I., Leung, H., Engelke, K., von Andrian, U. H., Deryugina, E. I., Strongin, A. Y., Bröcker, E. B. and Friedl, P,. (2003). Compensation mechanism in tumour cell

migration: mesenchymal-amoeboid transition after blocking of pericellular proteolysis. J. Cell Biol., v. 160, p. 267-277.

Wu, M. H., Urban, J. P. G., Cui, Z. and Cui, Z.F.. (2006). Development of PDMS microbioreactor with well-defined and homogenous culture environment for chondrocyte 3-D culture. Biomed. Microdev., v. 8, p. 331–340.

Wu, M. H.. (2009). Simple poly(dimethylsiloxane) surface modification to control cell adhesion. Surf. Interface Anal., v. 41, p. 11-16.

Wu, M-H., Huang, S-B., Cui, Z., Cui, Z. and Lee, G-B.. (2008). Development of perfusion-based micro 3-D cell culture platform and its application for high throughput drug testing. Sensors and Actuators B, v. 129, p. 231–240.

Xia, Y. and Whitesides, G. M.. (1998A). Soft lithography. A. R. Mat. Science, v. 28, p. 153-184.

Xie, J., MacEwan, M. R., Schwartz, A. G. and Xia, Y.. (2010). Electrospun nanofibers for neural tissue engineering. Nanoscale, v. 2, p. 35–44.

Xu, C. Y., Inai, R., Kotaki, M. and Ramakrishna, S.. (2004). Aligned biodegradable nanotibrous structure: A potential scaffold for blood vessel engineering. Biomaterials, v. 25, p. 877–886.

Yang, B. and Lin, Q.. (2007). Planar micro-check valves exploiting large polymer compliance. Sens. Actuators A, v. 134, p. 186-193.

Ye, Q., Zund, G., Benedikt, P., Jockenhoevel, S., Hoerstrup, S.P., Sakyama, S., Hubbell, J.A. and Turina, M.. (2000). Fibrin gel as a three dimensional matrix in cardiovascular tissue engineering. Eur. J. Cardiothorac. Surg., v. 17, p. 587–591.

Yeon, J. H. and Park, J. K.. (2007). Microfluidic cell culture systems for cellular analysis. Biochip. J., v. 1, p. 1727.

Yuan Wen, B. S.. (2009). Microfluidic and microscale cell cultures for High-throughput cell-based assays and bioprocess Development. Dissertation Presented in Partial Fulfillment of the Requirements for the Degree Doctor of Philosophy in the Graduate School of The Ohio State University.

Zaari, N., Rajagopalan, S. K., Kim, S. K., Engler, A. J. and Wong, J. Y.. (2004). Photopolymerization in microfluidic gradient generators: microscale control of substrate compliance to manipulate cell response. Adv. Mater. V. 16, p. 2133–2137.

Zaman, M. H., Trapani, L. M., Sieminski, A. L., Mackellar, D., Gong, H., Kamm, R. D., Wells, A., Lauffenburger, D. A. and Matsudaira, P.. (2006). Migration of tumour cells in 3D matrices is governed by matrix stiffness along with cellmatrix adhesion and proteolysis. Proc. Natl. Acad. Sci. USA, v. 103, p. 10889-10894.

Zhao, X. M., Xia, Y. and Walker, G. M.. (1996). Fabrication of three-dimensional micro-structures: Microtransfer molding. Adv. Mater., v. 8, p. 837-840.

Ziaie, B., Baldi, A., Lei, M., Gu, Y. and Siegel, R. A.. (2004). Hard and soft micromachining for BioMEMS: review of techniques and examples of applications in microfluidics and drug delivery. Adv. Drug. Deliv. Rev., v. 56, p. 145-172.

Zisch, A. H., Schenk, U., Schense, J. C., Sakiyama-Elbert, S. E. and Hubbell, J. A.. (2001). Covalently conjugated VEGF--fibrin matrices for endothelialization. J. Control. Release, v. 72, p. 101-113.